COMPARISON OF SYNCHRONOUS CHARGE TRAPPING AND VARIABLE EXHAUST VALVES IN A TWO-STROKE ENGINE

A Thesis

Presented in Partial Fulfillment of the Requirements for the

Degree of Master of Science

with a

Major in Mechanical Engineering

In the

College of Graduate Studies

University of Idaho

By

Andrew Hooper

June 2013

Major Professor: Karen DenBraven, Ph.D.

Authorization to Submit Thesis

This thesis of Andrew Hooper, submitted for the degree of Master of Science with a major in Mechanical Engineering and titled "COMPARISON OF SYNCHRONOUS CHARGE TRAPPING AND VARIABLE EXHAUST VALVES IN A TWO-STROKE ENGINE," has been reviewed in final form. Permission, as indicated by the signatures and dates given below, is now granted to submit final copies to the College of Graduate Studies for approval.

Major Professor _____ Date _____
Karen DenBraven, Ph.D.

Committee Member _____ Date _____
Daniel Cordon, Ph.D.

Committee Member _____ Date _____
David McIlroy, Ph.D.

Department Administrator _____ Date _____
John Crepeau, Ph.D.

Discipline's College Dean _____ Date _____
Larry Stauffer, Ph.D.

Final Approval and Acceptance by the College of Graduate Studies

_____ Date _____
Jie Chen, Ph.D.

Abstract

This thesis covers the methods, testing results, and analysis of operating characteristics for comparing a two-stroke engine equipped with parallel rotary synchronous charge trapped (PR-SCT) to an engine with variable exhaust port valves. Data were collected in six configurations of exhaust port geometries, two variable exhaust valve variations and four PR-SCT variations. The use of non-objective based testing provides in a high quantity of data, which are collected in a systematic manner.

This thesis is intended to provide the background of the two-stroke scavenging process so that the reader will be able to interpret the phenomenon observed. Parameters and basic models for the scavenging process are presented. Additionally the role and effect of the tuned exhaust pipe in a two-stroke engine is explained.

Performance parameters such as brake mean effective pressure (BMEP), brake specific fuel consumption (BSFC), and emissions production indicate that the traditional exhaust valves provide the greatest benefit. Performance of the PR-SCT system improves as engine speed is raised, approaching that of the variable exhaust valve. Analysis reveals that the valve does not seal off the cylinder well enough to trap the charge, leading to little improvement in trapping efficiency. Methods for measuring trapping efficiency are explored for use in future testing.

Acknowledgements

I have many people to thank for providing me the opportunity to complete this research; firstly, Dr. Karen DenBraven, my major professor, for providing funding to me via the National Institute for Advanced Transportation Technologies (NIATT). In addition to my research, funding and advice have been provided to the Clean Snowmobile Challenge Team for all five years of my involvement. I would also like to thank my committee members Dr. David McIlroy and Dr. Dan Cordon for reviewing my work. Dr. Cordon also provided me with a large amount of insight to engine operation and testing procedures. I am grateful for the two-stroke engine knowledge that the engineers at Bombardier Recreational Products have given me. Special thanks goes to my peers in the University of Idaho Clean Snowmobile Challenge team. Alex Fuhrman, Dylan Dixon, Nick Harker, Sam Smith, Peter Britanyak, Neil Miller, Jeremy Nichols, and Dillon Savage are on a long list of an even larger group of engineers that I have had the pleasure of working with. Lastly I want to thank my family, Gary, Melanie, and Woody Hooper, for supporting me though my stay at the University of Idaho, encouraging my advanced education, and providing numerous entertaining weekends.

Table of Contents

List of Figures

List of Tables

List of Equations

Definition of Terms

AFR	Air Fuel Ratio
BDC	Bottom Dead Center
BMEP	Brake Mean Effective Pressure
BSFC	Brake Specific Fuel Consumption
CE	Charging Efficiency
CFD	Computational Fluid Dynamics
CO	Carbon Monoxide
CO_2	Carbon Dioxide
EC	Exhaust port Close
EMM	Engine Management Module
EO	Exhaust port Open
EPA	Environmental Protection Agency
HC	Hydrocarbons
HCCI	Homogeneous Charge Compression Ignition
IA	Fuel Injection Angle
IMEP	Indicated Mean Effective Pressure
m_{ar}	Mass of fresh Air charge that is Retained from previous cycle
m_{as}	Mass of fresh Air charge Scavenged into cylinder
m_{ex}	Mass of Exhaust charge that is retained

m_{ref}	Mass Reference charge
m_{tas}	Mass of Trapped fresh Air Scavenged charge
m_{tr}	Mass of Trapped charge
NO_x	Oxides of Nitrogen
O_2	Oxygen (molecular)
PPM	Parts Per Million
PR-SCT	Parallel Rotary Synchronous Charge Trapping
RAVE	Rotax Adjustable Variable Exhaust
RPM	Revolutions Per Minute
SC	Short Circuit ratio
SCT	Synchronous Charge Trapping
SE	Scavenging Efficiency
SR	Scavenging Ratio
TC	Transfer port Close
TDC	Top Dead Center
TE	Trapping Efficiency
TO	Transfer port Open
UICSC	University of Idaho Clean Snowmobile Challenge team
WOT	Wide Open Throttle
wrt	With Respect To

φ Equivalence ratio (phi)

λ Normalized AFR (lambda)

1 Introduction

1.1 Motivation

Across the globe, compact, simplistic power sources are required for use in transportation, recreation, and other uses. In the United States, internal combustion engines using the Otto cycle (four-stroke) are the primary engine of choice for transportation. These engines are often characterized by low emissions and high efficiency. Another common type of engine is the two-stroke engine. They are synonymous with high emissions and poor fuel efficiency. These power plants are frequently used in power sports and implements, where they are favored for their high power density, which is producing high power for their weight. Within these same markets, four-stroke engines, much like those used for transportation, are also employed for increased fuel economy and reduced emissions output.

In other parts of the world, such as Asia, two-stroke engines are more widely used for transportation. Low cost manufacturing, low maintenance, and compact design make these engines very popular for scooters and small three-wheeled vehicles. However, these engines produce large amounts of harmful exhaust emissions and have high fuel consumption.

This study was conceived to test the effectiveness of the parallel rotary synchronous charge trapping (PR-SCT) at improving the operating characteristics of a two-stroke engine. Improving the mid-range power, fuel economy, and emissions of two-stroke engines can help to improve air quality in third world countries and improve the performance of recreational vehicles in other regions.

At a much higher level, the impact of man-made carbon burning device, such as internal combustion engines, is having a definite impact on the Earth. A decade of controversy has left much of the public skeptical of the reality of global warming or climate change, and of whether they have been caused by human activities [1]. The consequences of a climate shift can have disastrous effects on life on earth. The possibility of climate change, as well as the finite amount of available fossil fuels, supports the importance of the conservation of fossil fuels. Efforts to reduce carbon emissions are a small step in long-term sustainability.

1.2 Research goals

Previous testing of the PR-SCT has shown that the prototype engine produces less power at higher speeds than a stock engine [2]. This testing was performed without the use of a tuned exhaust pipe. The particular goals of this study are to determine whether the PR-SCT engine can improve mid-range performance characteristics of a two-stroke engine while using a tuned exhaust system. The PR-SCT design patent is held by the University of Idaho, and positive research data are necessary for the engine to be marketable. By comparing the mid-range operating characteristics to a conventional variable exhaust valve system, the possible success of the PR-SCT in the market can be determined.

2 Two-stroke engines

The low mechanical complexity of the two stoke engine comes at a cost. This cost is less control of fluid movement through the engine. The exhaust and intake processes of an Otto cycle engine are separated by different strokes of the piston. In contrast, most two-stroke engines' intake process is enveloped by the exhaust process. Starting at top dead center (TDC), the power stroke continues until exhaust port opening (EO). The exhaust port remains open while the transfer ports open (TO) as the piston continues to move downward. Fresh air charge is introduced through the transfer ports, which in turn assists in expelling the exhaust products through the exhaust port. During this process, mixing of the fresh and exhaust charges occurs (this will be discussed further in Section 2.2). Intake and exhaust continue through bottom dead center (BDC). When the piston starts moving upward, the transfer ports closes (TC) first (at the same piston height in which it opened), followed by exhaust port closure (EC). Once the exhaust port is closed, the charge compression begins. Ignition occurs before TDC, causing fuel combustion and concluding the cycle. Figure 1 illustrates how the scavenging process is overlapped by the exhaust process. Scavenging is a term used to describe the process of air being introduced into the combustion chamber [3].

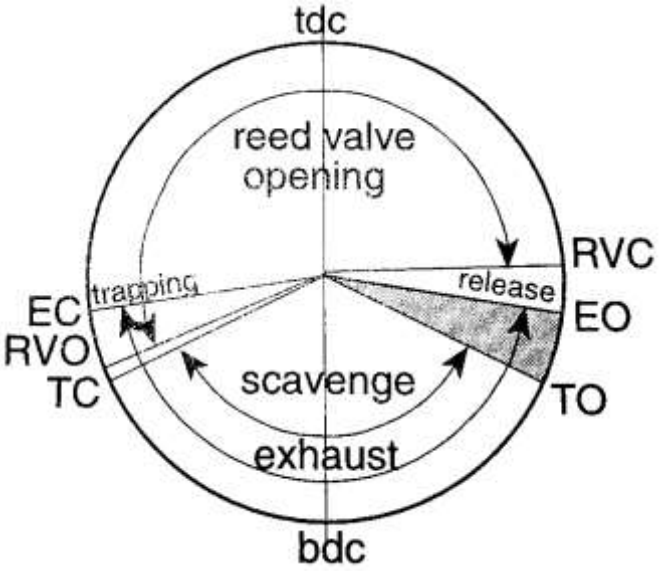

Figure 1: Cycle diagram for typical port timing of a two-stroke engine [3]

2.1 Gas flow through the cylinder

Since the exhaust and intake processes occur at the same time, the charge retained in the cylinder for combustion is not pure intake charge. It is also true that the fluids flowing out the exhaust port are not purely products of combustion. On the trapping of the charge, the trapped gas mass (m_{tr}) is composed of a combination of the following gases: trapped scavenged charge (m_{tas}), combusted exhaust charge (m_{ex}), unburned air charge retained from the previous cycle (m_{ar}). This is illustrated in Equation 1.

$$m_{tr} = m_{tas} + m_{ex} + m_{ar}$$

Equation 1: Composition of trapped charge is an internal combustion engine

To quantify gas flows through the cylinder, engine developers use a common set of nomenclature: scavenging ratio, scavenging efficiency, trapping efficiency, and charging efficiency.

2.1.1 Scavenging Ratio

The scavenging ratio (SR) is used to quantify the amount of air that is introduced into the cylinder. It is defined as the mass of air scavenged (m_{as}) into the cylinder over the reference air mass (m_{ref}) as shown in Equation 2. The reference mass is the mass of air required to fill the entire cylinder volume at ambient temperature and pressure.

$$SR = \frac{(m_{as})}{(m_{ref})}$$

Equation 2: Definition of air scavenging ratio for an two-stroke engine

Qualitatively the SR is the amount air is being consumed by the engine. The SR is limited by an intake throttle to allow lower air consumption, and therefore control the power output of the engine. The SR does not have an upper limit of a value of one. It is possible that the air entering the cylinder would more than fill the cylinder volume at ambient conditions.

2.1.2 Scavenging Efficiency

The scavenging efficiency (SE) depicts the portion of trapped charge that is fresh scavenged charge. It is defined as the mass of trapped scavenged charge divided by the mass of trapped charge as shown in Equation 3.

$$SE = \frac{(m_{tas})}{(m_{tr})}$$

Equation 3: Definition of air scavenging efficiency for an internal combustion engine

The SE identifies how well the scavenging process is able to expel all of the charge from the previous cycle. The SE does have a maximum value of one.

2.1.3 Trapping Efficiency

In most cases the mass of air delivered to the cylinder is not equivalent to the mass of air trapped in the cylinder. This can be characterized by the trapping efficiency (TE) at a given operating condition. The trapping efficiency is defined as the ratio of the trapped, scavenged charge mass (m_{tas}) to that of the scavenged charge mass as shown in Equation 1 [3].

$$TE = \frac{(m_{tas})}{(m_{as})}$$

Equation 4: Definition of air trapping efficiency for an internal combustion engine

It is important to note that the term in the numerator does not include any gases retained in the cylinder from the previous cycle. The portion of the scavenged air that is not retained in the cylinder is short-circuited into the exhaust. This fraction could be calculated as one minus TE. Since the scavenged charge is usually a mixture of air and fuel, the short-circuited charge is a major contributor to harmful exhaust emissions and poor fuel economy. For example, under normal operation conditions a snowmobile engine will short-circuit 20-40% of the fuel [4]. Figure 2 shows data from testing using throttle body fuel injection. With this type of fuel injection system the scavenged charge is a homogeneous fuel-air mixture.

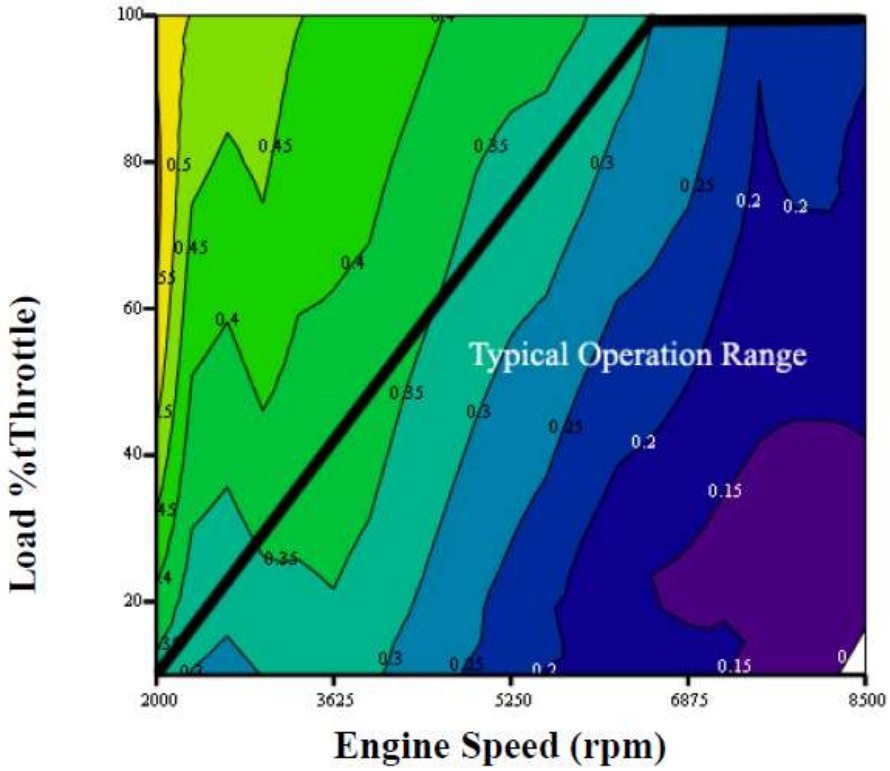

Figure 2: Fraction of fuel short-circuited vs. engine speed and throttle position for a throttle body injected snowmobile engine [4]

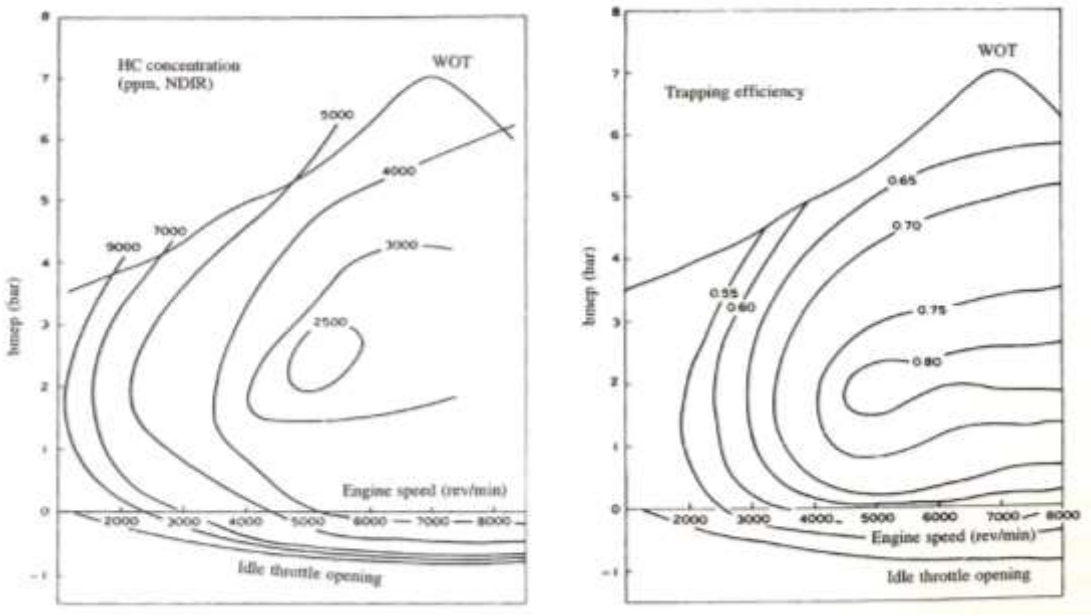

Figure 3: Hydrocarbon emission and trapping efficiency vs. engine speed and load for a carbureted two-stroke engine [5]

Figure 3 illustrates the very strong correlation between trapping efficiency and hydrocarbon (HC) emissions [5]. HC concentration of 2500 parts per million (PPM) correlates closely to 80% trapping efficiency (20% short-circuited) and 5000 PPM HC correlates closely to 60% trapping efficiency (40% short-circuited). The trapping efficiency can be roughly approximated by the fraction of fuel short-circuited in Figure 2.

2.1.4 Charging efficiency

The charging efficiency (CE) is a measure of the ability to trap fresh charge in the cylinder. The definition of CE is the mass of trapped scavenged charge divided by the reference mass charge as shown in Equation 5. This proportion is also equal to the SR multiplied by the TE.

$$CE = \frac{(m_{tas})}{(m_{ref})} = SR * TE$$

Equation 5: Definition of charging efficiency for an two-stroke engine

The CE generally has a positive relationship to the brake mean effective pressure (BMEP) of homogeneous charge combustion engines. BMEP is a measure of the brake work output of the engine normalized to the size and speed of the engine. BMEP is defined in Equation 6, where N_r is the number of crank rotations for one engine cycle (N_r=1 for two-stroke engines). [6]

$$BMEP = \frac{Work\ output}{Engine\ Swept\ Volume * Engine\ Speed/N_r}$$

Equation 6: Definition of brake mean effective pressure (BMEP) for an internal combustion engine

2.2 Scavenging of a Two-Stroke

In order to expel the exhaust gases and introduce the fresh charge at the same time, the fresh charge will push (or displace) the exhaust charge out through the exhaust port. The design of

the transfer ports is a critical aspect of optimizing this process. Most modern crankcase scavenged two-stroke engines use ports designed for a loop-scavenging strategy. Figure 4 shows general flow lines for the scavenging flow of a Curtis-Type loop scavenging strategy [4].

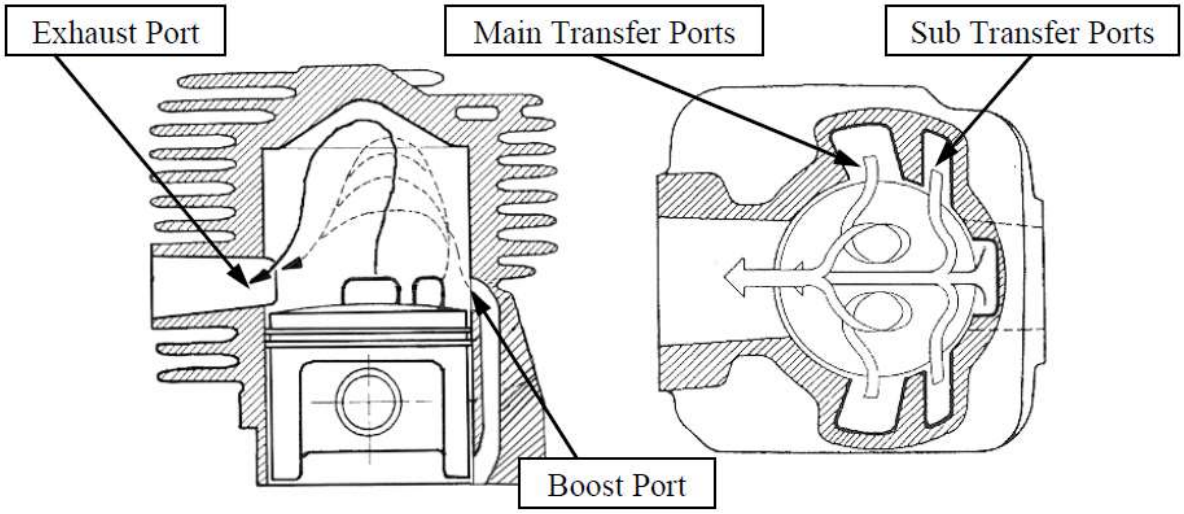

Figure 4: Schematic of in-cylinder flows for a Curtis-Type loop-scavenged two-stroke engine [4]

The ratio and efficiency terms explained earlier give insight to the composition of charges in the cylinder, but no insight as to the mechanisms which govern those results. There are two fundamental models, perfect displacement and perfect scavenging, that are used to describe to simplest possible outcomes of the SE and TE based on the SR. It is important to notice that these models use the SE, TE, and SR on a basis of volume rather than mass.

2.2.1 Perfect Displacement Scavenging

Under the conditions of the perfect displacement model, the fresh scavenge charge and exhaust charge do not mix. The fresh charge volume displaces the exhaust volume to the point where the exhaust volume is completely removed from the cylinder. If more volume is

scavenged than the cylinder holds (i.e. SR>1), then the excess fresh charge will be short-circuited [7] [3] [5] [6]. A graph of this model is shown in Figure 5.

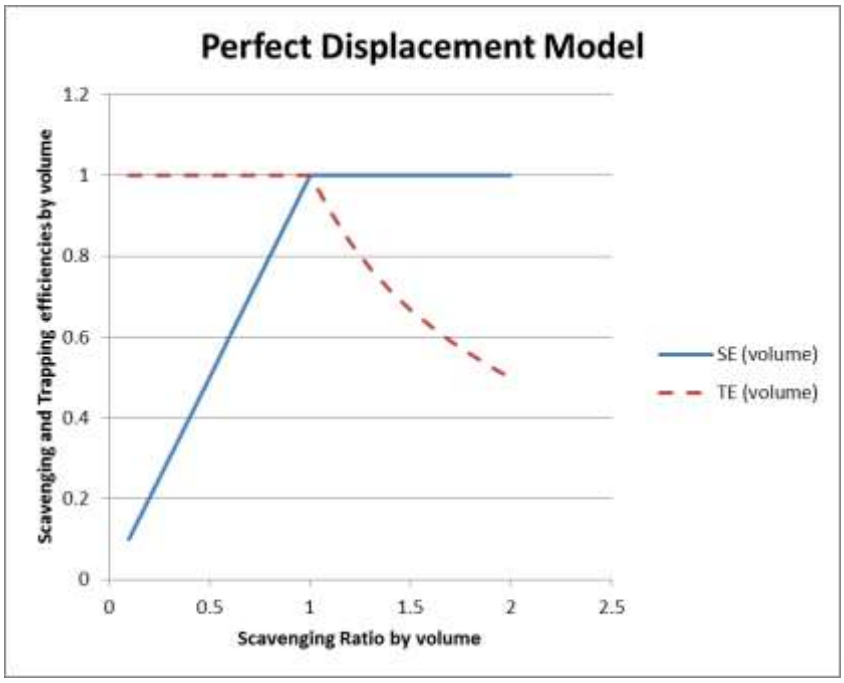

Figure 5: Scavenging and trapping efficiencies for the perfect displacement model of two-stroke engine cylinder scavenging

2.2.2 Perfect Mixing Scavenging

The perfect mixing model states that the fresh charge volume mixes instantaneously with the volume in the cylinder. The exhausting volume is identical in composition to the charge in the cylinder [3] [6] [7] [5]. This model results in scavenging and trapping efficiencies much lower than those of the perfect displacement model. Figure 6 illustrates the perfect mixing scavenging model. Since these two models do not intersect at any point, it is not possible for both to be valid for any particular engine.

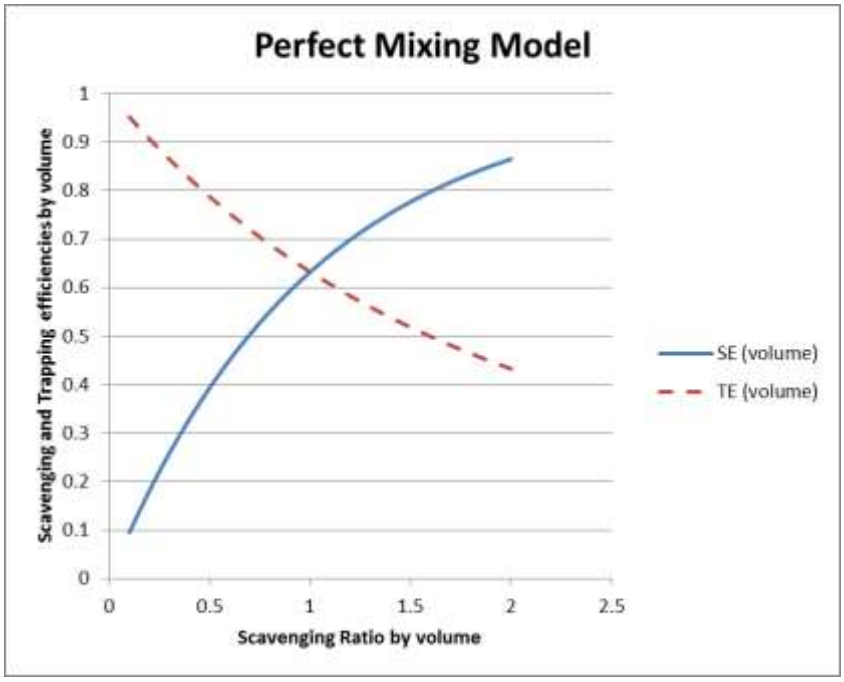

Figure 6: Scavenging and trapping efficiencies for the perfect mixing model of two-stroke engine cylinder scavenging

2.2.3 Experimental Data

To determine the validity of either of these models, they are compared to experimental data obtained from laboratory tests. In Figure 7 and Figure 8**,** the yam12 and yam14 data sets represent loop scavenged cylinder designs for a single cylinder Yamaha engine [3]. These Yamaha cylinders will more closely represent values from a snowmobile engine than the other engines. It is easy to see that neither the perfect displacement nor the perfect mixing models accurately predict these results.

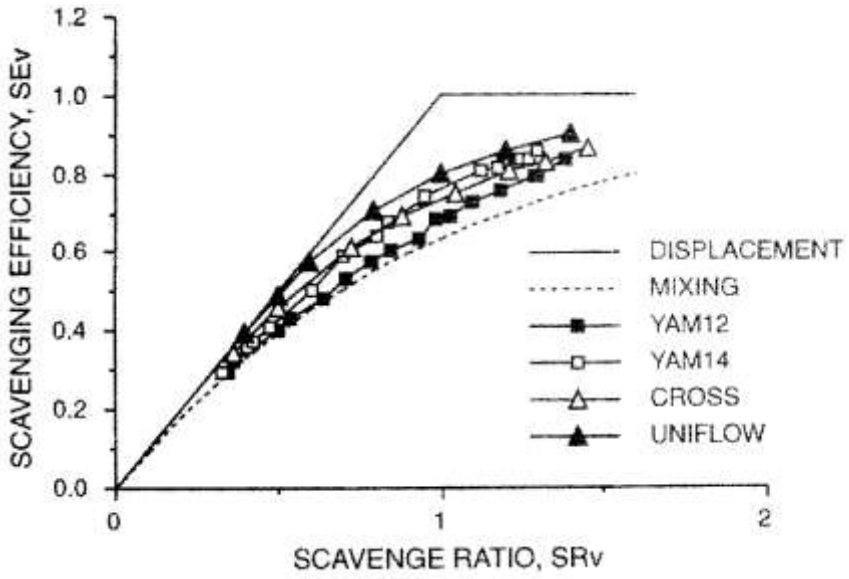

Figure 7: Experimental data of SE vs. SR for two-stroke engines [3]

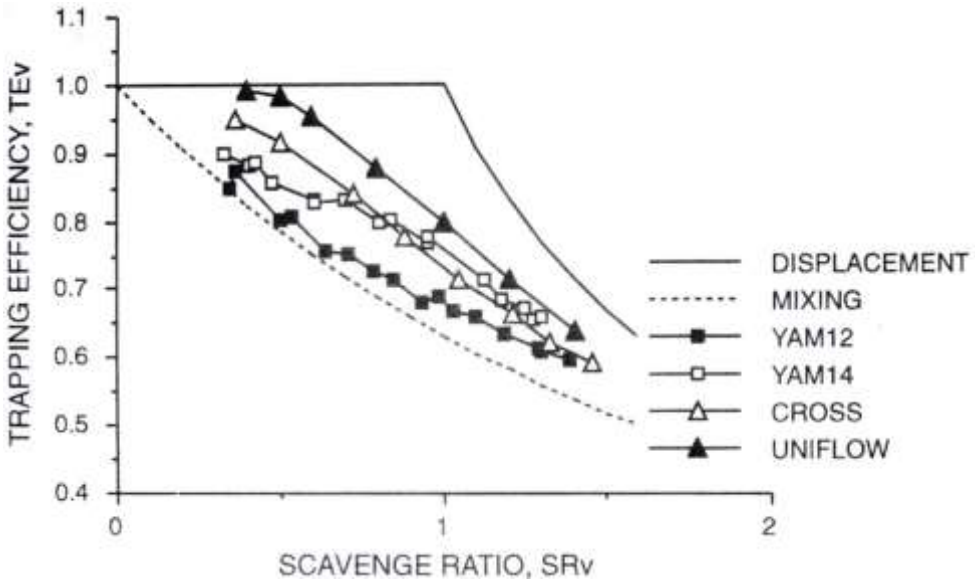

Figure 8: Experimental data of TE vs. SR for two-stroke engines [3]

Blair [3] also reports data in the form of purity at the exhaust port vs. SR, shown in Figure 9. Purity is the concentration of fresh scavenge charge in the sampled fluid. A perfect scavenging model would show a step from zero to one hundred percent at an SR value of

one, and a perfect mixing model would show a plot very similar to that of the curve for SE in Figure 7.

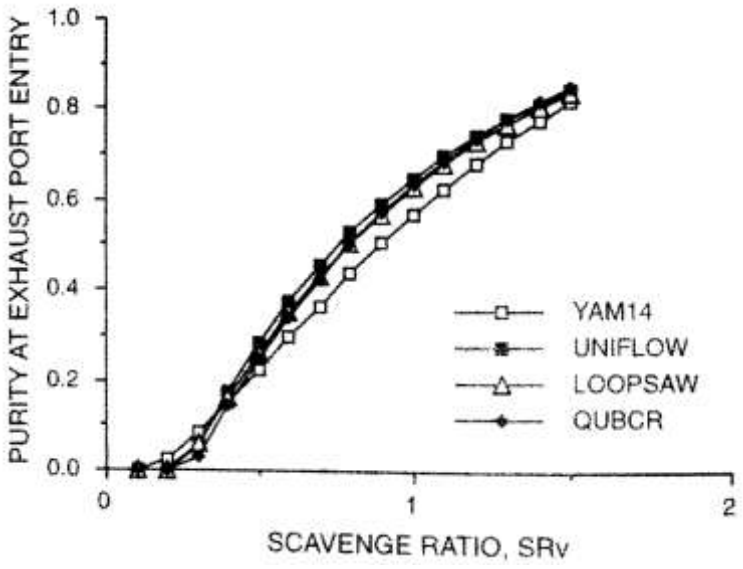

Figure 9: Experimental data for purity at exhaust port vs. SR in a two-stroke engine [3]

2.2.4 Other Models

To better approximate the experimental data, a more accurate model is needed. Many models are proposed by Blair [3]and Heywood [5]. These are essentially best fit techniques, combining displacement, mixing, and short-circuiting in different proportions as the scavenging ratio varies. One model, developed in 1977, is shown in Figure 10. It provides a visualization of how the scavenged charge is introduced into the cylinder [6]. Computational fluid dynamics (CFD) has become a valuable tool for the designer as it is used to simulate the flows through a proposed cylinder configuration.

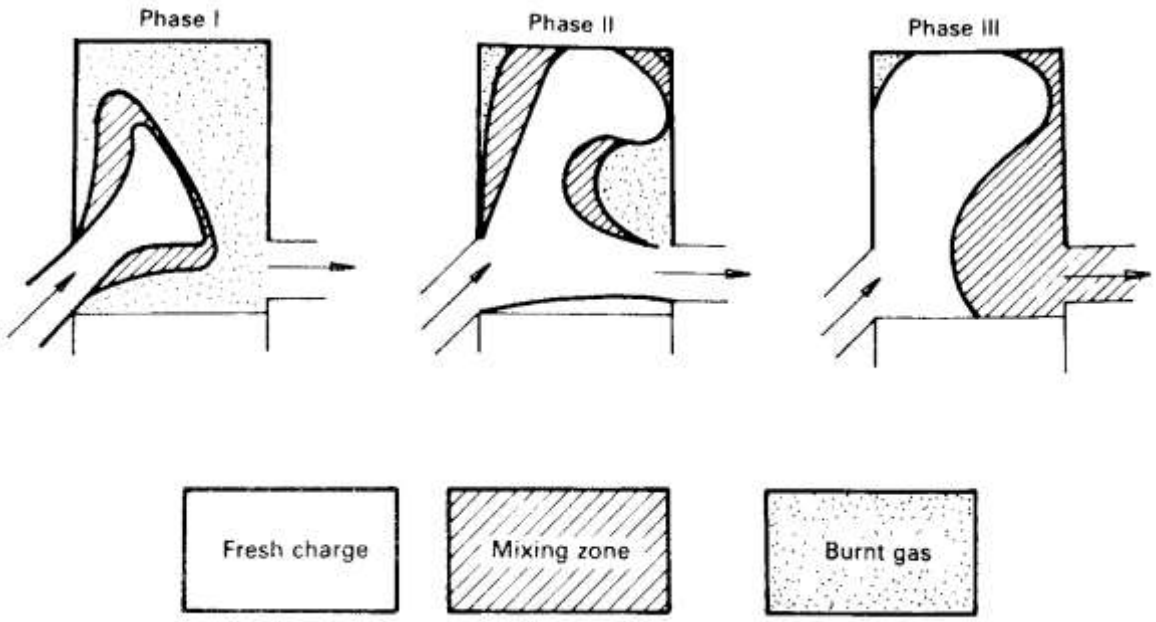

Figure 10: Visual model of the scavenging process in a two stroke engine [6]

One major conclusion can be drawn from the information presented on scavenging: it is possible that either a large portion of the scavenging charge mass will short-circuit through the exhaust port, or a large amount of charge from the previous cycle will be retained. In actuality, it is a combination of the two.

2.3 Tuned Exhaust Pipe

The tuned exhaust pipe, or exhaust system, is commonly used to achieve high power output of two-stroke engines. The tuned pipe works on the principal of high pressure waves passing through a pipe or duct with changing cross sectional area, causing a pressure wave to be reflected back to the cylinder. The pressure wave emitted through an exhaust port can reach over two atmospheres in pressure. If a positive pressure wave passes through a diverging section (i.e. the area is increasing in direction of travel) then a negative pressure wave is reflected opposite to the direction of travel of the initial wave. As a result, flow is induced in

the same direction as the original pulse. Similarly, a wave traveling through a converging duct will reflect a positive wave, inducing flow opposite to the direction of the original wave.

A tuned pipe has two basic features to improve the SR and TE. First, a diverging section assists the exhaust process. By inducing flow out of the cylinder, the time required to evacuate the exhaust products and introduce the fresh scavenge charge is reduced. The tuned pipe also includes a converging section. This prompts flow back into the cylinder later in the cycle, thus increasing the mass trapped in the cylinder. The timing of the suction and trapping pulses are dependent on the length of the sections and the speed at which the pulses travel. Positive pressure waves travel at a speed slightly higher than the local speed of sound and the negative pulses travel slightly slower than the local speed of sound [3]. Equation 7 shows the equation for the local speed of sound in an ideal gas [8].

$$v_s = \sqrt{\gamma * g_c * R * T}$$

Equation 7: Equation for local speed of sound for ideal gases

The general concept of the tuned exhaust pipe is illustrated in Figure 11. The dark band "A" is the transmitted high pressure pulse; "B" is the reflected low pressure pulse; and "C" is the reflected high pressure pulse. For a given initial pulse strength and gas temperature, the response of the tuned pipe stays nearly constant with respect to (wrt) time. As the engine speed varies; however, the pressure response changes wrt crank angle. In Figure 11 the vertical axis is labeled as time, and has markers for positions of the piston. These only coincide at a certain speeds of the engine.

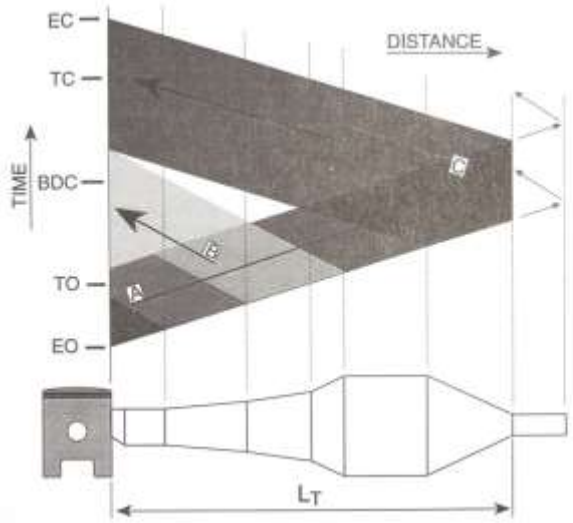

Figure 11: Optimum pressure wave timing in a tuned exhaust system [3]

When the engine is not operating at the design speed of the tuned exhaust, the TE is significantly reduced. Pressure traces at the exhaust port and combustion chamber are used to determine flow patterns through the engine. Figure 12 illustrates the pressure traces of an engine running at its designed speed. The low pressure region has a pressure ratio below one, and occurs over a broad crank angle range. The high pressure trapping pulse peak occurs about 20° before EC. A reverse flow of gases, induced by the trapping pulse, causes charge to flow back into the cylinder from the exhaust ducting. This causes the cylinder pressure to continue to rise through EC. At the point of EC the pressure ratio is over 2.5. Figure 13 shows the same engine operating lower than its designed operating speed. Many differences can be noticed between the exhaust traces at the two operating speeds. Most notably, the trapping pulse comes back to the exhaust port too early. As a result, the charge flows back out the exhaust port and the pressure ratio drops to roughly 2 at the time of EC. The lower trapping pressure correlates to a lower TE. The reduction of the low pressure region indicates that the SR is greatly reduced. As noted in section 2.2, the SE is likely to decrease as the SR decreases.

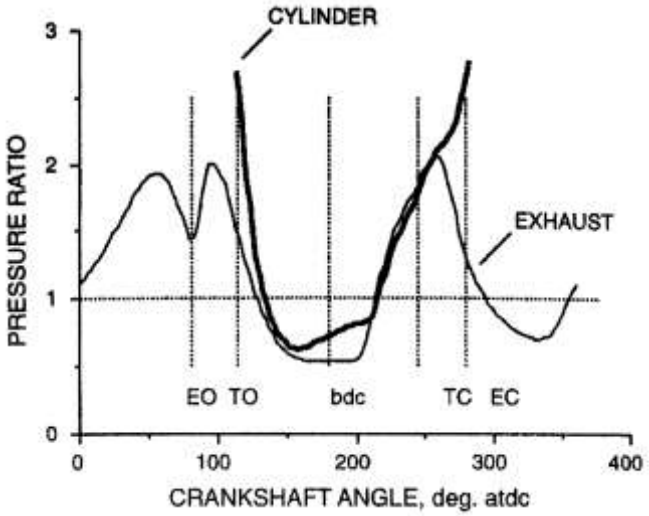

Figure 12: Pressure trace of a single cylinder engine at tuned speed [3]

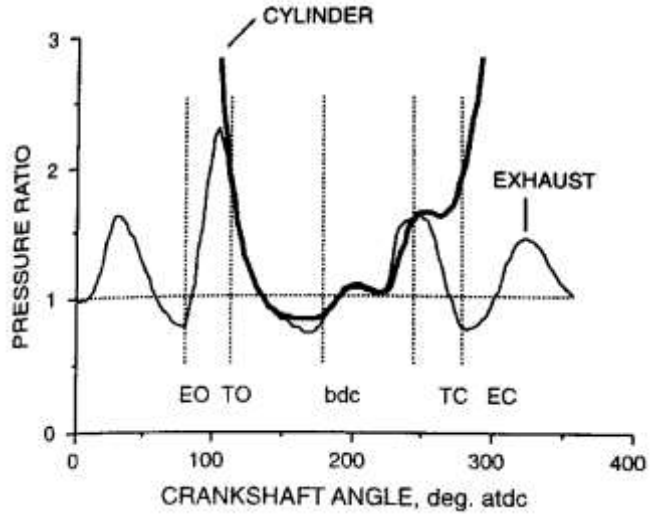

Figure 13: Pressure trace of a single cylinder engine at 80% of tuned speed [3]

2.4 Variable Exhaust Valves

Modern designs have made vast improvements in short-circuited fuel-air charge over older systems. Variable exhaust port valves are widely used to improve the low to mid-range operating characteristics of the engine. Variable exhaust port valves allow the height of the exhaust port to be altered during engine operation. A common mechanism in snowmobile engines is a guillotine-style sliding valve. The slide lowers the port height during low speed

operation, and raises the port for high speed operation. Figure 14 shows a pressure trace of an engine operating at low speed with the exhaust control valves in the lowered position. As expected, the EO and EC are much closer to the TO and TC respectively in this configuration. The exhaust valve allows for a longer expansion before EO. A longer power stroke and lower pressure pulse emanating from the exhaust port result. In turn, the tuned pipe effect is reduced, which is favorable while operating away from the tuned speed. Earlier EC provides higher trapped volume and therefore higher TE.

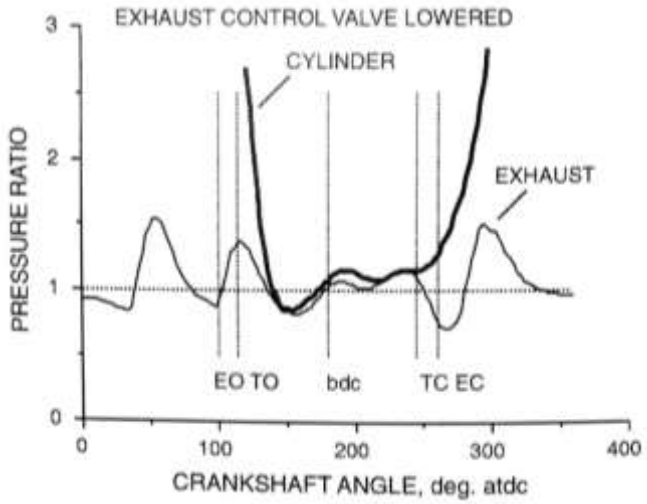

Figure 14: Pressure trace of a single cylinder engine at 70% of tuned speed [3]

2.5 Direct Fuel Injection

Another technology that has advanced two-stroke engines is direct fuel injection (DI). DI systems inject a precise amount of fuel directly into the combustion chamber. This advance over other fuel injection and carburetion systems provides the ability for the fuel to be introduced into the cylinder later in the cycle so that the short-circuited charge does not contain fuel. Currently, Orbital and E-TEC injection systems are used in marine engine and other applications for improved fuel economy and emissions compliance.

2.6 Synchronous Charge Trapping

Synchronous charge trapping (SCT), also known as asymmetrical exhaust port timing, is another developing technology that shows promise for improving efficiency and emissions output of two-stroke engines. SCT allows for EO and EC to occur at different piston positions. Designs using this concept have been created by Boyesen Engineering, Lotus Engineering, and the University of Idaho.

The system being developed by Lotus deserves extra attention. The engine package dubbed "the Omnivore" is a venture into broad range homogeneous charge compression ignition (HCCI). It is called the Omnivore because the platform is capable of operating on a multitude of fuels without hardware change. HCCI uses premixed fuel ignited by the compression in the cylinder rather than a spark ignition. HCCI generates very high rates of heat release at piston TDC, resulting in high thermal efficiencies. The omnivore engine uses SCT to control the amount of retained exhaust charge which is regulated to create the conditions necessary for HCCI to occur. In upcoming years this technology may be seen in automotive applications [9]. The Omnivore engine illustrates the asymmetry of the exhaust port in Figure 15.

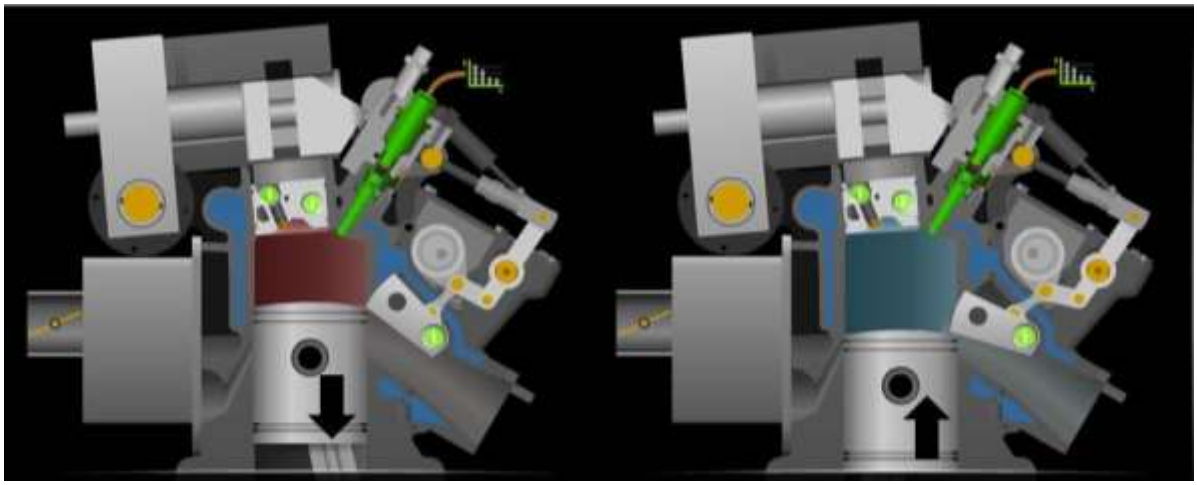

Figure 15: Cross section of the Lotus Omnivore with early (high) exhaust port opening (left image), and early (low) exhaust port closure (right image) occurring in one cycle [10]

The first system created at the University of Idaho, as well as those by Boyesen and Lotus, use a reciprocating valve to lower and raise the exhaust port during the cycle. These systems are further explained in Peter Britanyak's thesis [11]. A second SCT engine was next created and patented at the University of Idaho, which allowed for higher operational speed by using rotary valves rather than a reciprocating design [12].

2.6.1 The PR-SCT System

The PR-SCT prototype was designed and manufactured at the University of Idaho between September 2010 and May 2011 by a group of four engineering students as their Senior Capstone Design project [13]. The system is retrofitted to a Rotax 600 engine from a Ski-doo snowmobile. The original engine specifications are listed in Table 1 [14]. All of the original geometries were retained except for the exhaust ports, which were fitted with the rotary valve system.

Engine Cycle	Two-Stoke
Cooling	Liquid
Cylinder(s)	2
Bore	72 [mm]
Stroke	73 [mm]
Displacement	593 [cc]
Intake	Cylinder Reed Valve
Scavenging	Loop (Curtis-Type)
Rated speed	8000 [RPM]
Rated Power	82 [kW] (97 Nm @ 8000 RPM)

Table 1: Stock Rotax 600 specifications

The prototype rotating assembly is made of stainless steel for high temperature operation and the valve housings are machined from aluminum alloys. The prototype is pictured in Figure 16 with one of the inserts removed for viewing. The power take off (PTO) cylinder valve can be seen without the counterbalance weights attached. A unique drive system was developed in order to turn the valve assembly counter-crank-wise, and allows for the phase between crank and valve shaft to be adjusted during operation.

Figure 16: PR-SCT engine with one insert removed

3 Belt drive remodel

Since the prototype was first finished in 2011, the belt drive system has been a source of several mechanical issues. The original system is pictured in Figure 17. This system was unable to hold the crossbar firmly in place and had difficulty tensioning the belt. The second system was built to handle these issues. This system can be seen in Figure 18. One noticeable feature is the threaded holes in the back plate. This allowed the adjuster bar to be locked into place. In addition, the idler pulleys were held in place by two bearings rather than one to better distribute the load on the idler shaft [2]. A tensioning system in the lower part of Figure 18 improved the consistency of belt tension. The second system still had some drawbacks. Adjusting the advance was time consuming: the idler pulleys spun at double the crank speed, and the manufacturing process resulted in the pulleys being non-concentric about their shaft, causing oscillatory valve shaft accelerations.

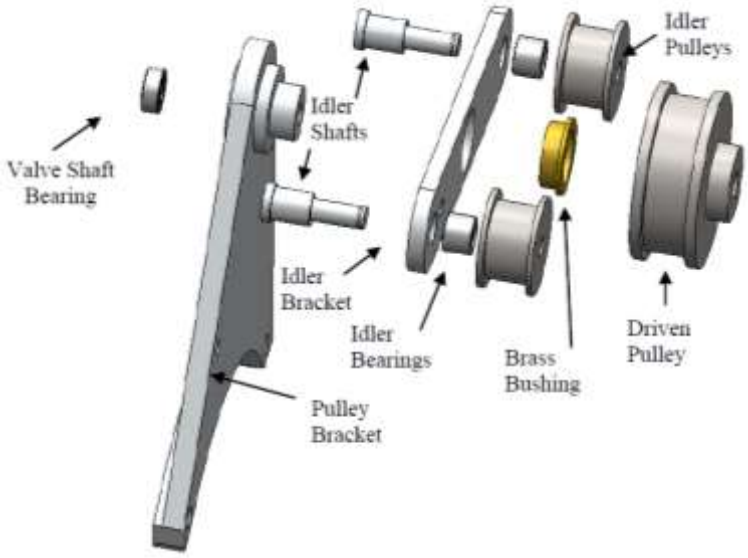

Figure 17: Original belt drive design for the PRSCT system [2]

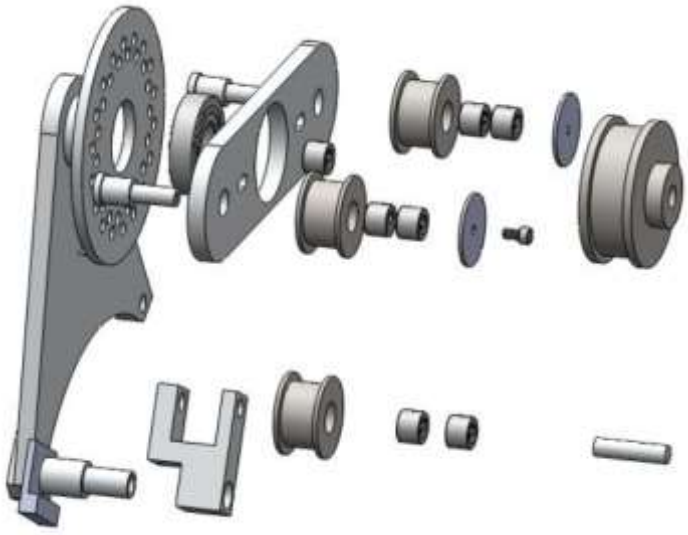

Figure 18: Second design of a belt drive for the PRSCT system [2]

The third belt drive system was developed to reduce the time to adjust, minimize oscillations, and reduce the number of parts in the system. By decoupling the two idler pulleys, the tensioning function can be performed by one idler with the advance adjustment set by the other. A solid model of the system is shown in Figure 19. The pulleys are fastened to the short shafts, which in turn ride on sealed ball bearings in the control arms. This greatly improves the radial tolerances. The control arm pairs are fastened together with flathead screws via a small block. The adjusting arm pair controls the timing of the valve shaft via a turnbuckle, and the tensioning arms tighten the belt by use of a coil spring tied from the arms to main plate. Both of the control arm pairs pivot on a common shaft, provided by a 5/16” shoulder bolt. The completed system is pictured in Figure 20.

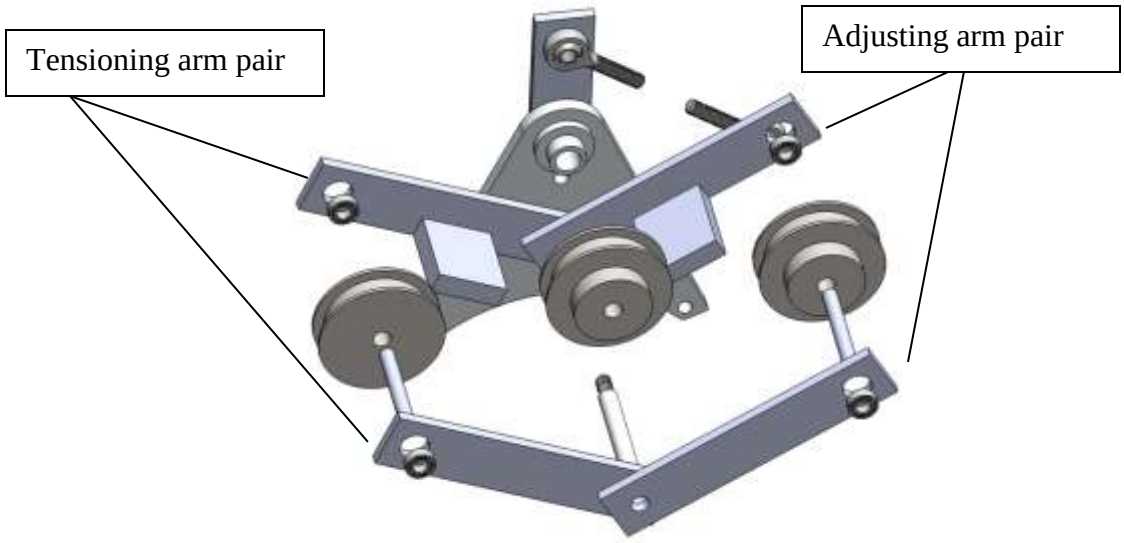

Figure 19: Third belt drive design for the PRSCT system

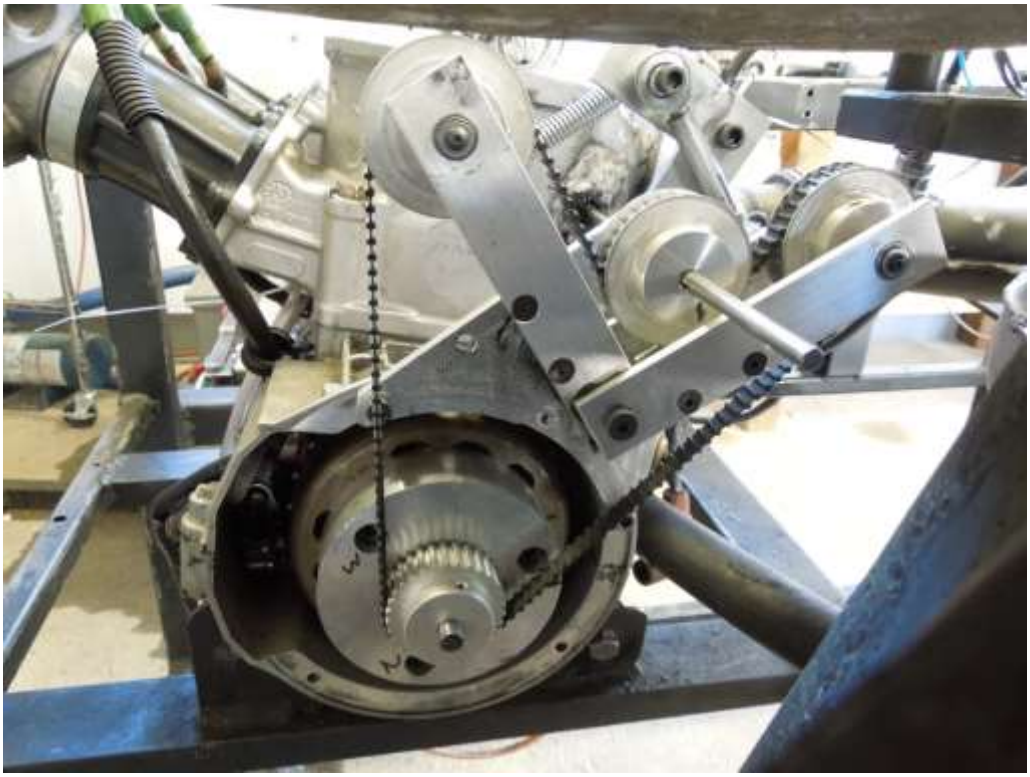

Figure 20: Manufactured prototype of the third belt drive design

4 Testing

4.1 Testing Equipment

4.1.1 Dynamometer

Engine speed and load are controlled by a Borghi-Saveri, model: FE-260-S eddy-current dynamometer. The dynamometer is controlled by a SuperFlow data collection and control system. This system uses the SuperFlow WinDyn software which operates on a Microsoft Windows platform in conjunction with a handheld controller. The system is capable of controlling the load on the engine while recording and displaying engine speed, torque output, and any other information provided by other sensors connected to the interface.

4.1.2 Fuel consumption

Fuel flow measurement is accomplished by a 710 Max Machinery fuel measurement system. Fuel consumption is used to compare engine efficiency as reported by brake specific fuel consumption (BSFC). BSFC is measured as the fuel used to produce a measured amount of shaft work, commonly reported in units of g/kW-hr. The fuel flow is also required to calculate the mass flow of emissions.

4.1.3 Exhaust gases

Exhaust gas concentrations are measured by a MEXA-584L Horiba portable emissions analyzer. This analyzer is capable of measuring carbon dioxide (CO_2), carbon monoxide (CO), oxygen (O_2), nitrogen oxides (NO_x), and HC concentrations. These values are reported in percent by volume, and can be logged at a rate of one sample per second for durations in one minute increments.

4.2 Hardware configurations

Two similar engines are used for the comparison. The first is a production Rotax engine with Rotax adjustable, variable exhaust (RAVE) 2 valves. The second is the PR-SCT engine. These two engines are operated in multiple configurations to provide a comparison of RAVE and PR-SCT performance. All configurations use the same fuel injectors, exhaust system, and intake system. The first configuration is the production engine with the RAVE 2 in the upward position, and the second with the RAVE 2 in the fully lowered position. The third hardware configuration is the PR-SCT engine without the valves installed in the exhaust housing. The final configurations are the PR-SCT with the rotary valves in set at varied timing, with configuration four being the most advanced and configuration six being the most retarded. The advanced timing will result in the valve closing the exhaust port earlier in the cycle, while the retarded setting will close the port later in the cycle. A summary of the hardware configurations is shown in Table 2.

Configuration	Description
1	Production engine, RAVE 2 up
2	Production engine, RAVE 2 down
3	PR-SCT, Valves Removed
4	PR-SCT, EC at 120° before TDC
5	PR-SCT, EC at 113° before TDC
6	PR-SCT, EC at 109° before TDC

Table 2: Description of hardware configurations for the engine testing

4.3 Testing Methods

The methods used for this testing reflects the anticipated effects of the system. By using the PR-SCT in conjunction with a tuned exhaust system mid-range performance should be noticeably improved. Without a tuned exhaust system this PR-SCT prototype is prone to have inadequate scavenging [2]. This is due to the port geometries of the stock Rotax

engine. With high ports, the SR and TE are reliant on the tuned pipe response. The early EO and early EC, provided by SCT, in conjunction with a tuned exhaust system show great promise for improving operating characteristics of the engine in a wide range of speeds. At low speeds, SCT allows for early exhaust port closure to increased trapped scavenged charge. At high speeds, SCT vavle effect can be reduced by retarding the valve while the tuned exhaust pipe performs the duty of trapping the scavenged charge. At mid-range speeds, the charge trapping works in conjunction with the tuned exhaust to trap cylinder charge at higher volume and pressure by closing the exhaust port shortly after the trapping pulse from the tuned exhaust encounters the cylinder.

Since the high speed operation should not be influenced greatly by the SCT it is not examined during this testing. The mid-range speeds are emphasized during the testing, as low speed testing has been conducted without a tuned pipe by Austin Welch [2]. The standard operating conditions of the engine are tested by using two of the mode points from the standard EPA (Environmental Protection Agency) test, and the performance is tested by acquiring maximum torque at the same mode point engine speeds.

4.3.1 Mode Points

The standard for testing exhaust emissions from snowmobiles was developed by the Southwest Research Institute. The test consists of five modes which represent the duty cycle of the engine during operation. The weighting and definition of the mode points are shown in Table 3. The E-score is the resulting calculation of emissions output, shown in Equation 8, where HC, CO, and NO_x values are computed as the sum of the brake specific output of the constituent at each mode multiplied by the respective mode weighting [15]. Modes three

and four have been selected as the targeted test points. For this engine, mode three is approximately 32 Nm @ 6000 RPM, and mode four is approximately 18.5 Nm @ 5200 RPM.

Mode Point	1	2	3	4	5
Speed (% of Rated)	100	85	75	65	Idle
Torque (% of Rated	100	51	33	19	NA
Weighting (%)	12	27	25	31	5

Table 3: The five modes used for the EPA emissions test of snowmobile engines

$$E\text{-}Score = \left[1 - \frac{HC + NO_x - 15}{150}\right] * 100 + \left[1 - \frac{CO}{400}\right] * 100$$

Equation 8: E-score calculation for snowmobile engines

To reduce time spent in testing, the mode points are not directly obtained. Rather, a throttle position is held constant for all configurations at a test point. Only fuel injection angle and quantity are varied at the set points of throttle position and RPM. Furthermore, to obtain a greater amount of knowledge about the engine operation at these points, objective calibration is not used. Instead, data are collected at varied injection angle and quantities. These data can reveal more information about the effect that the variables have on the operation of the engine.

4.3.2 Maximum Torque

To measure performance increases, the maximum torque is acquired from each configuration. The maximum torque is targeted at two points: 5200 RPM and 6000 RPM, both at wide open throttle (WOT). Calibrating for maximum torque requires the engine to operate fuel rich. Increasing the fueling will increase the BMEP slightly until the mixture

becomes very rich, at which point BMEP will decrease. A problem arises that the variation in BMEP is very little over a wide range of fueling values. Increasing the fueling by a large factor may result in a slight increase in power, but will result in high fuel consumption and emissions production. To remove this unwanted side-effect, fueling values were chosen based on the following criteria: a fuel injection angle (IA) value of 230° BTDC and injection quantity set such that the CO concentration is approximately 2% by volume.

4.3.3 Naming convention

To identify an individual sample of collected data a simple naming convention was developed that will be referred to for the duration of this thesis. There are four identifying numbers for every point. The first is the hardware configuration. Refer to Table 2 for a description of each hardware configuration. The second is the operating point. The reasoning for choosing these points was previously explained and the chosen points are shown in Table 4.

Operating Point	Engine Speed (RPM)	Throttle Position
1	5200	10%
2	6000	20%
3	5200	100%
4	6000	100%

Table 4: Description of operating points for engine testing

The third number is the injection angle. This value is set in the engine management module (EMM) and can be adjusted on the fly by the interface software. The fourth and final value is the injection quantity, which is also controlled by the EMM. For each combination of hardware configuration and first two operation points, a set of injection angles are selected and for those a range of injection quantity values are selected and divided into even increments. The fuel quantity extreme values are dictated by the following conditions: a lean

limit where torque output decreases to approximately 10% below its high value, and a rich limit at approximately three percent carbon monoxide concentration by volume in the exhaust. For the first configuration and operating point a grid of eight injection angles and eight fuel quantities was used. This resulted in 64 independent data points, which provide information on the effects of varying fuel injection angle and quantity. Although this returned a high resolution grid of data, it was very time consuming. To reduce time in the engine testing laboratory a grid of four injection angles by five injection quantities was used.

		Fuel Lean		λ		Fuel Rich
	150°	1	2	3	4	5
IA	170°	6	7	8	9	10
	190°	11	12	13	14	15
	210°	16	17	18	19	20

Table 5: Fuel calibration grid for twenty data points at a mode point during engine testing

The fuel injection timing and lambda ranges were defined for the grids as follows: the injection angles used ranged evenly between pre-determined early and late injection timings. These injection angles were 150, 170, 190, and 210 degrees before TDC. The lambda values comprised of five values within the suitable operating range for each injection angle. The lean limit of the range was defined as the point where a 10% loss of torque (compared to rich operation) occurred. The rich limit was defined as the point where 3% CO occurred.

4.4 Data Collected

A total of 256 data points were collected. These data populated the injection angle and quantity grids for all configuration/operation point configurations except for hardware configurations five and six at operating points two and four. A mechanical failure occurred during the testing, barring further data collection. Of the points collected, there were three points that are completely discarded. These were collected shortly after the engine was

started during that testing session. As a result the engine behaved differently due to its colder block and coolant temperatures. Additionally there were four points of invalid fuel flow values. For these points a fuel measuring system malfunction was caused by a plugged fuel filter. Due to this same problem fuel flow measurement was not recorded for hardware configurations one and two at operating points three and four. The data were collected and used to calculate performance parameters using Microsoft Excel. Mathwork's Matlab was used to plot them as visual aids.

5 Results

The results of the laboratory testing will be expressed in BMEP (in units of bar) to convey work output of the engine, BSFC (in units of kg/kW-hr) to convey the efficiency of the engine, HC and CO are reported (in units of g/kW-hr) for brake specific emissions, and the total exhaust emissions are reported in a dimensionless value equivalent to the negative impact on the E-score. At operating points one and two these results are plotted against the IA and lambda (λ). Lambda is defined as the ratio of measured air fuel ratio (AFR) and the known stoichiometric AFR of the fuel. The air fuel ratio is a measure of the mass of air and mass of fuel being burned (units of kg_{air}/kg_{fuel}). Lambda, therefore, does not have units. This ratio of AFRs is also often reported as the equivalence ratio (φ), which is the inverse of lambda [16]. Lambda is favored for use with internal combustion engines because it has the same sign sensitivity as AFR.

$$\lambda = \frac{AFR_{measured}}{AFR_{stoichiometric}} = \frac{1}{\varphi}$$

Equation 9: Equation for lambda and equivelance ratio

5.1 Efficiency

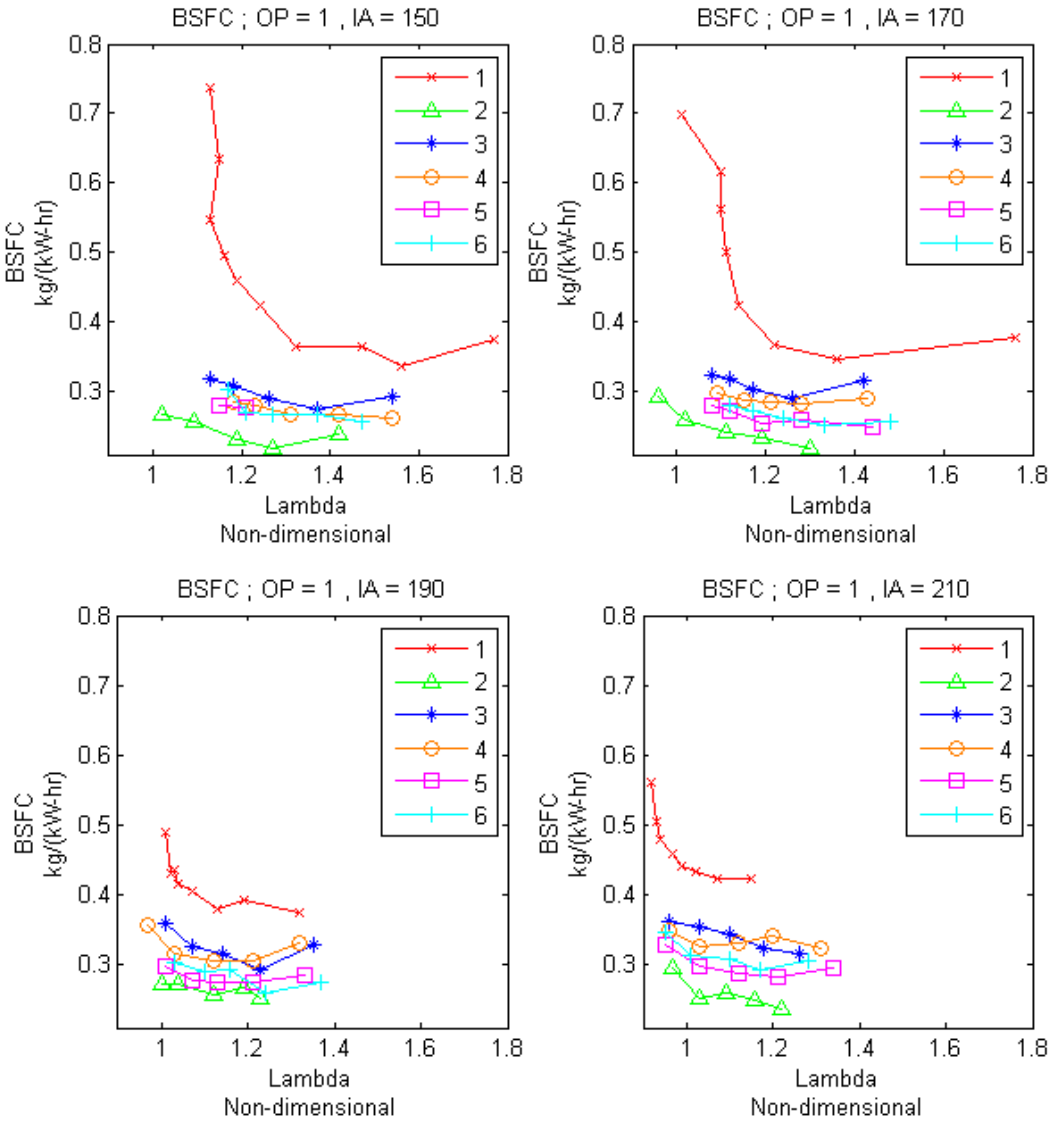

Figure 21: BSFC results for all configurations at operating point one

The results shown in Figure 21 depict a large improvement from configuration one to configuration two. Configuration one has the highest, and therefore the most unfavorable, fuel consumption while configuration two has the lowest. The best point for configuration two is 35% better than the best point of configuration one. The best point for a given

configuration occurs at the most favorable value of all injection timing and lambda calibrations. Although configuration three was anticipated to behave similarly to configuration one, it showed an improvement of 18% over configuration one.

The main points of interest are configurations four through six, as these are the PR-SCT configurations. These are compared to configuration three to quantify the effect of the trapping valve. Configurations four, five, and six have improvements of 4.6%, 8.9%, and 8.2% respectively over configuration three.

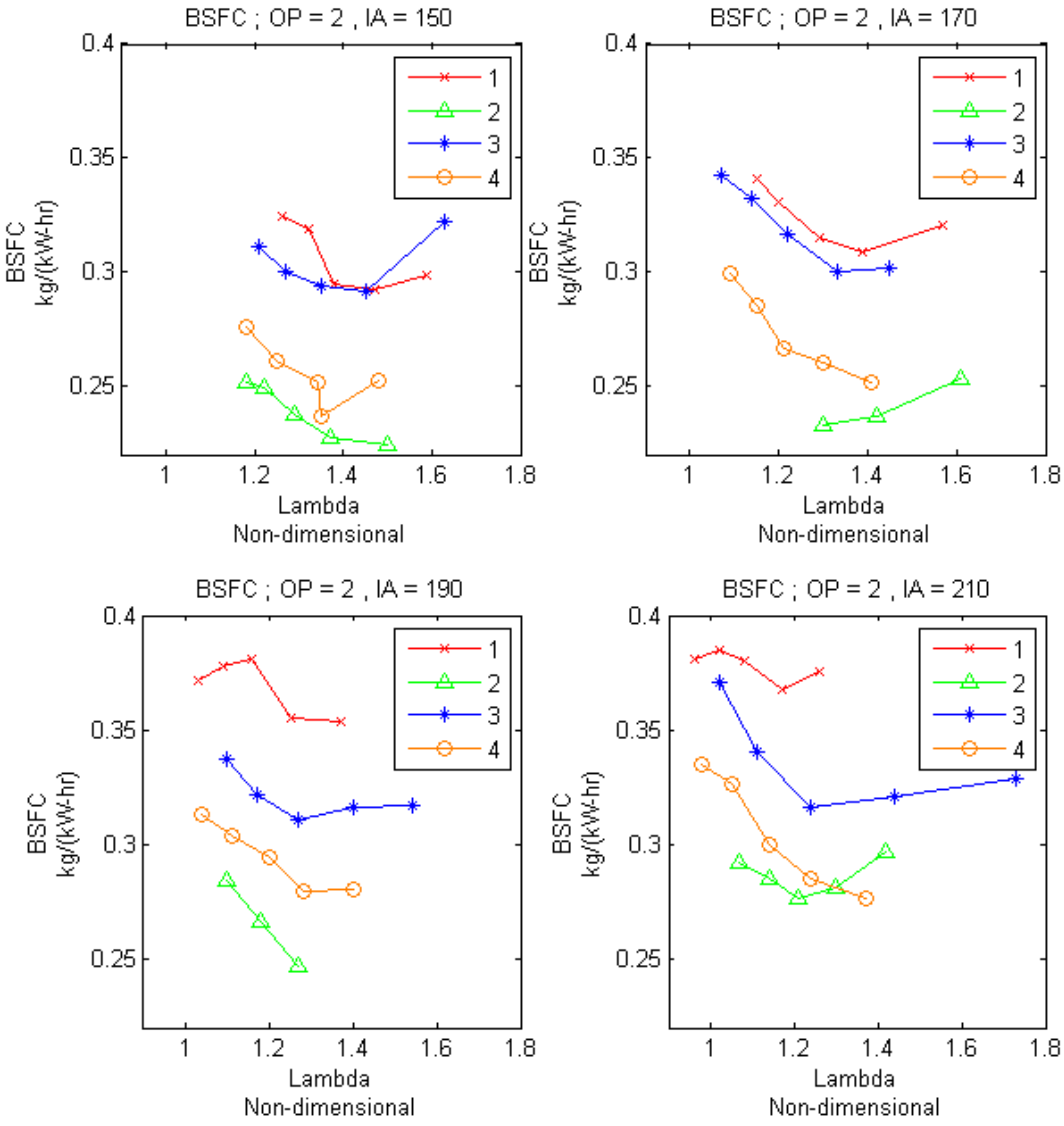

Figure 22: BSFC results for configurations one through four at operating point two

A slightly different story is conveyed at operating point two in Figure 22. Here the power valve shows a 23% improvement over the open port configuration (configuration one). The open port PR-SCT (configuration 3) has a minimum BSFC value nearly identical to that of configuration one, occurring at late injection angle. The early port close PR-SCT

configuration (configuration four) shows the best improvement at 19% over the open port PR-SCT configuration.

5.2 Emissions

5.2.1 HC

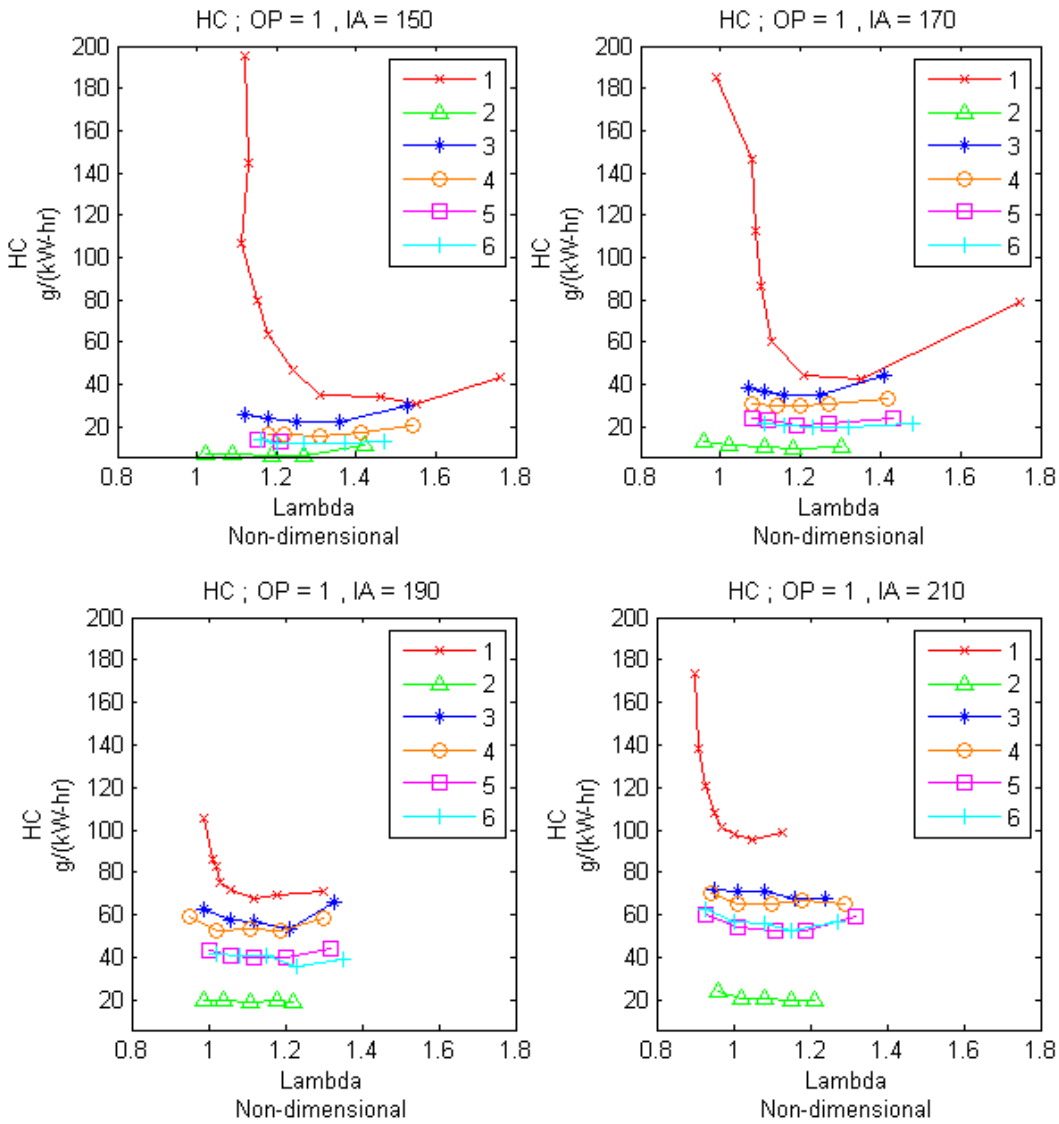

Figure 23: HC results for all configurations at operating point one

The HC emission results are similar to those of BSFC. Figure 23 shows the HC emissions at operating point one. As with BSFC, a lower value corresponds with a more desired result. Again the values are affected drastically by the presence of the power valve in configuration two. Configuration two boasts a 79% lower value than configuration one at their best points. Configuration three improves 28% over configuration one. The PR-SCT configurations (four, five, and six) achieve 29%, 42%, and 46% improvements respectively over configuration three. Since the HC emissions of a two-stroke engine primarily consist of short-circuited fuel mixture and the TE is increased as short-circuiting is reduced, it can be deduced that the TE is increased as the valve angle is retarded. The implications of this are discussed in

Conclusions.

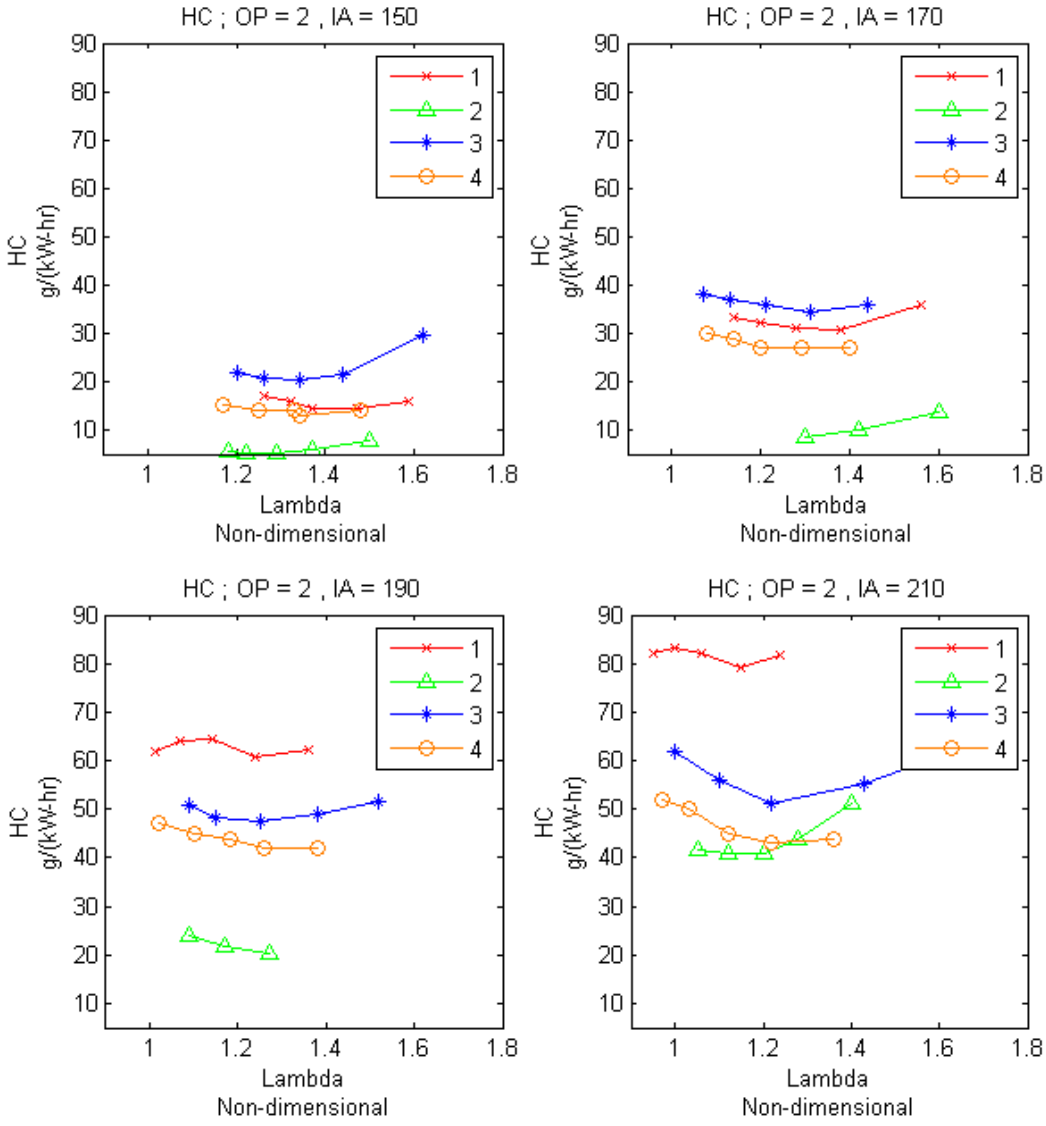

Figure 24: HC results for configurations one through four at operating point two

Figure 24 shows that the HC results from operating point two do not follow the same trends as operating point one. The improvement incurred by lowering the power valves is 63%. Configuration three is worse than configuration one, a 41% increase at their corresponding best points. And the PR-SCT valve in configuration four reduces the HC emissions by 36%

over configuration three. This further shows that the valve is increasing the TE, but not to the same extent as the power valve. Another interesting observation is the magnitude of variation as the IA is increased. Configurations one and two exhibit more dramatic increases in HC than configurations two and four do.

5.2.2 CO

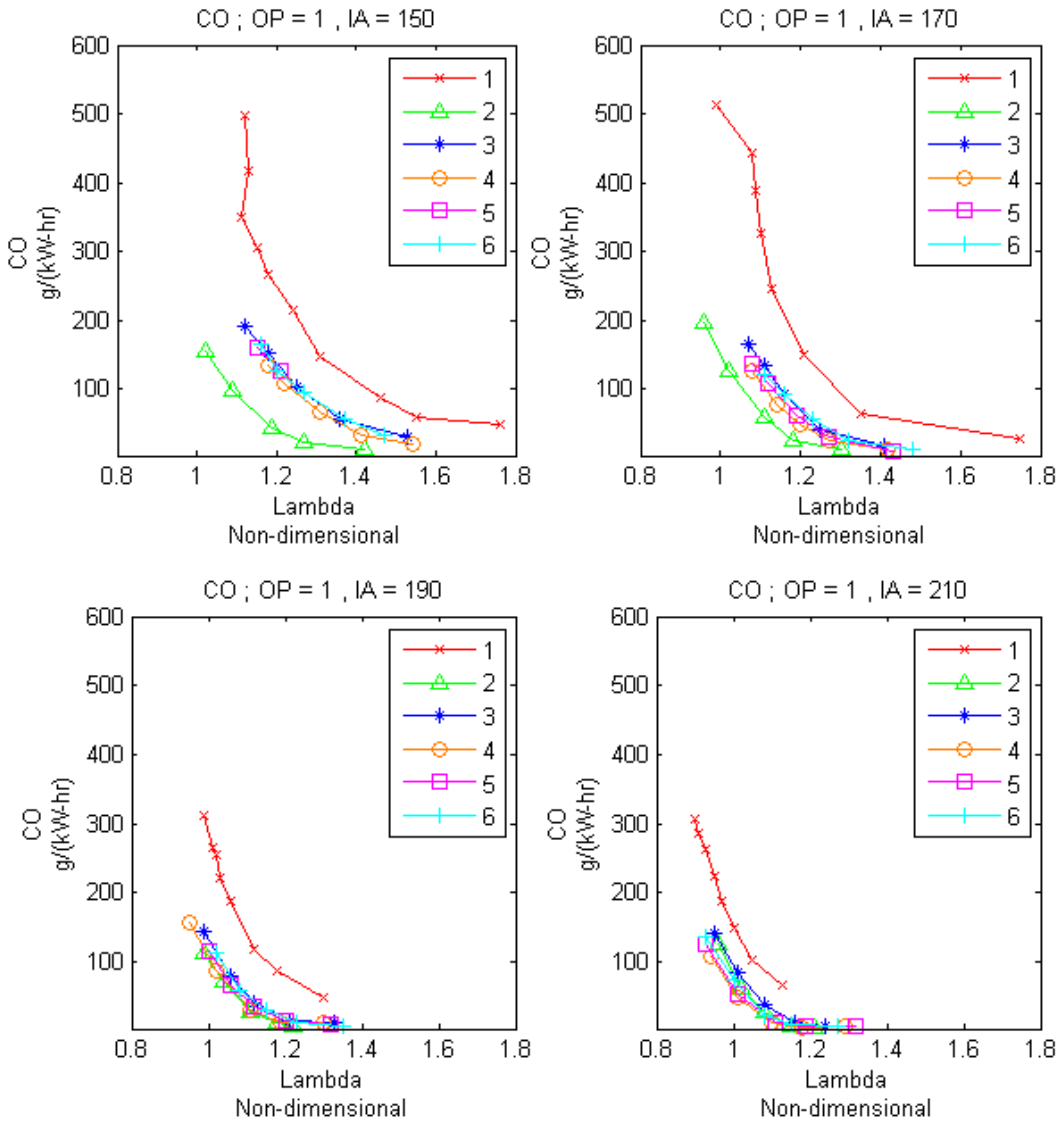

Figure 25: CO results for all configurations at operating point one

The CO emissions of an engine are a metric of combustion performance. High CO is a result of incomplete combustion. This incomplete combustion can be caused by low AFR, flame quenching, misfire, or other various factors [4]. The CO trends from the test data are depicted in Figure 25 and Figure 26. At operating point one; the CO emissions are cut by 87% with the introduction of the power valves. A 71% reduction is seen in configuration three compared to configuration one. The PR-SCT valves reduce the CO emissions in configurations four, five, and six by 30%, 24%, and 24% wrt configuration three. At operating point two, these trends change to 68% from configuration one to configuration two, 70% from one to three, and 22% from three to four.

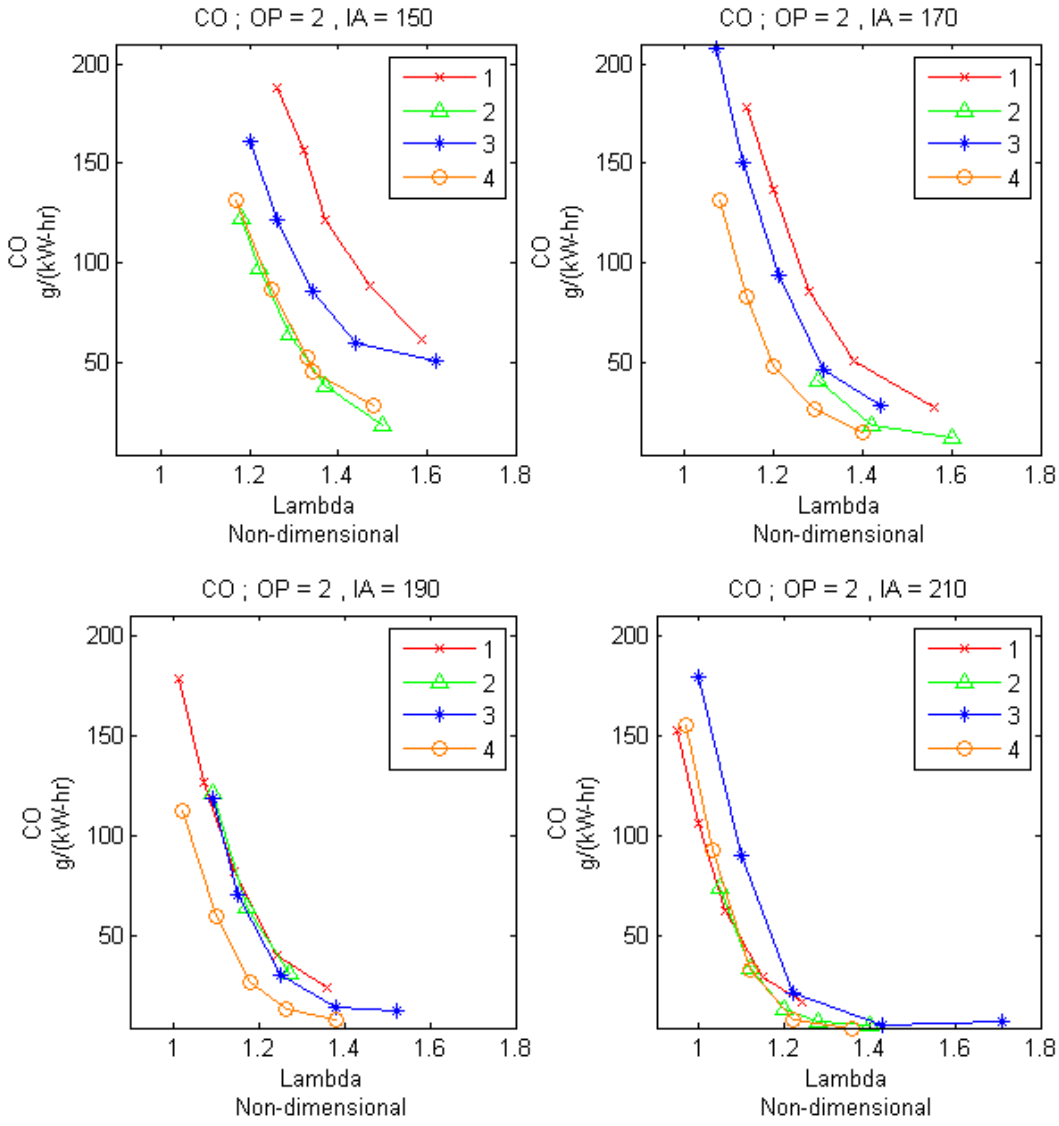

Figure 26: CO results for configurations one through four at operating point two

5.2.3 Total Emissions

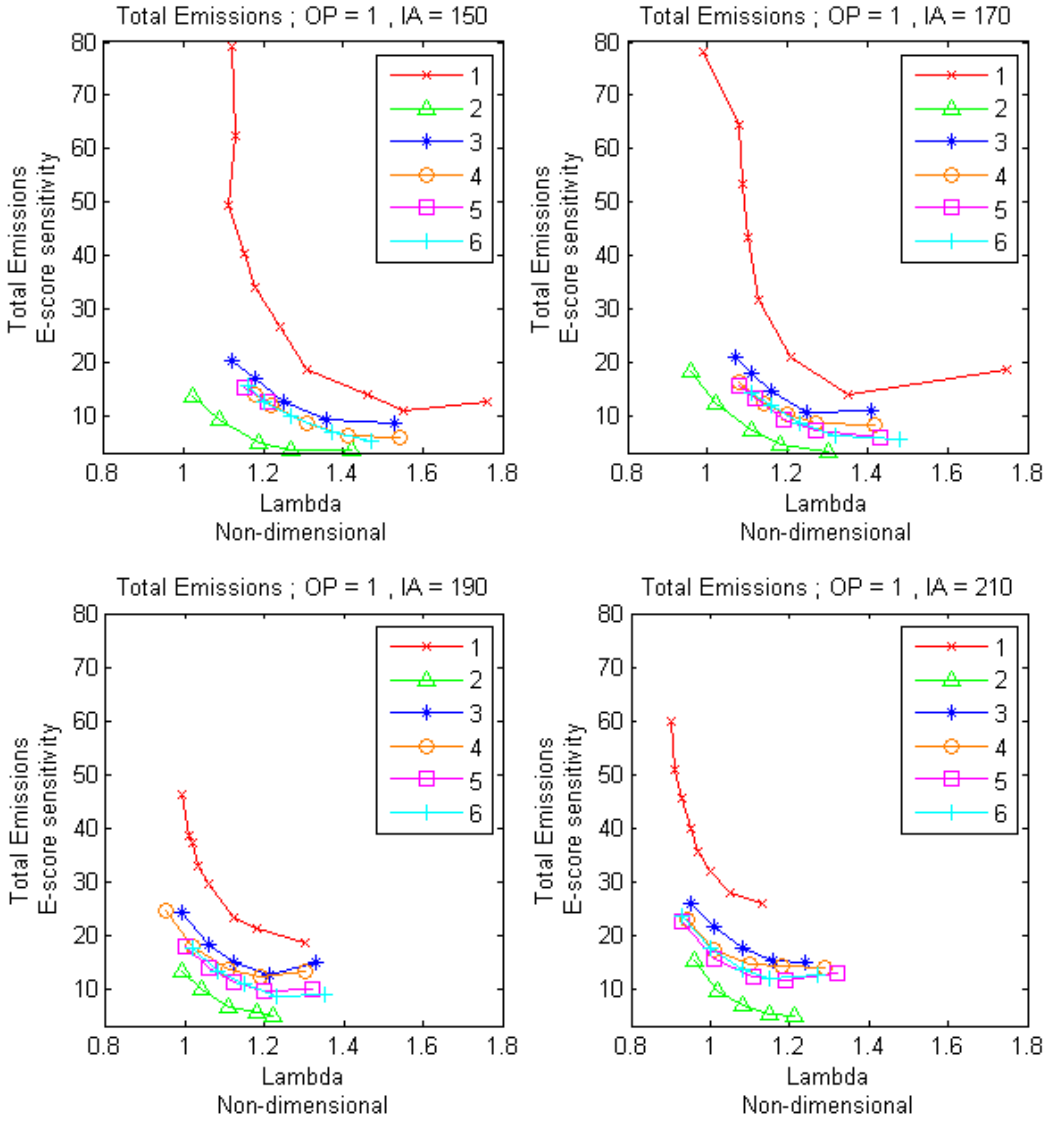

Figure 27: Total emissions results for all configurations at operating point one

The total emissions values depicted in Figure 27 and Figure 28 are based on the same function and method of emissions scoring done in the E-score testing. Configuration one is consistently the worst in this measure, and configuration two the best. At operating point one this correlates to a 70% improvement. A 21% improvement occurs between

configurations one and three. The PR-SCT valve incurs 33%, 33%, and 40% improvements over configuration three for configurations four, five, and six respectively. At operating point two, the reduction caused by the power valves is lessened to 55%, configuration three returns 13% higher total emissions than configuration one, and configuration four is 38% lower than configuration three. These data show a drop in total emissions of over 30% caused by the PR-SCT valve. Although the best value achieved for configuration three is higher than the best value achieved by configuration one, it can be noted that configuration three consistently produces lower emissions at other operating conditions.

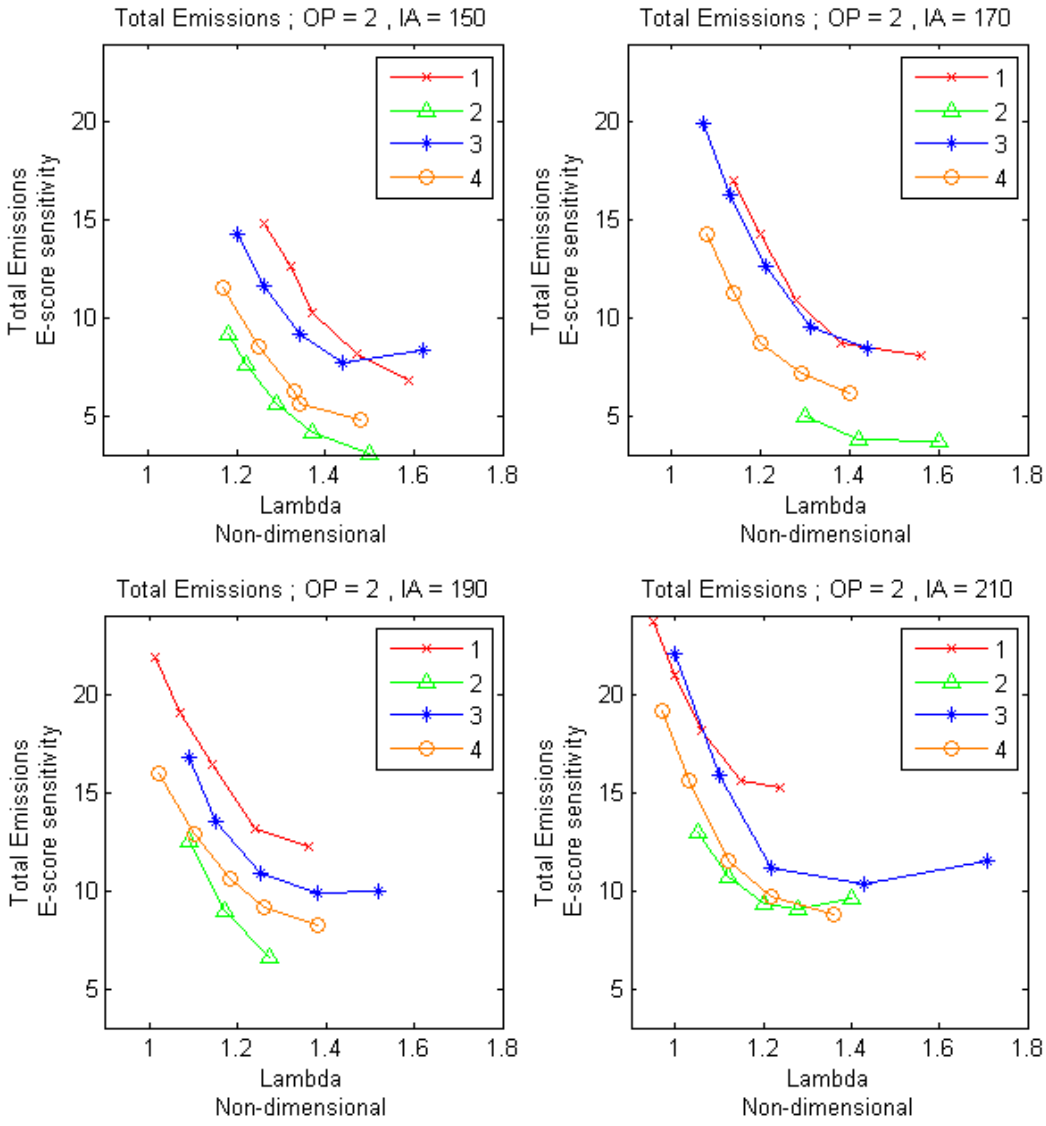

Figure 28: Total emissions results for configurations one through four at operating point two

5.3 Power output

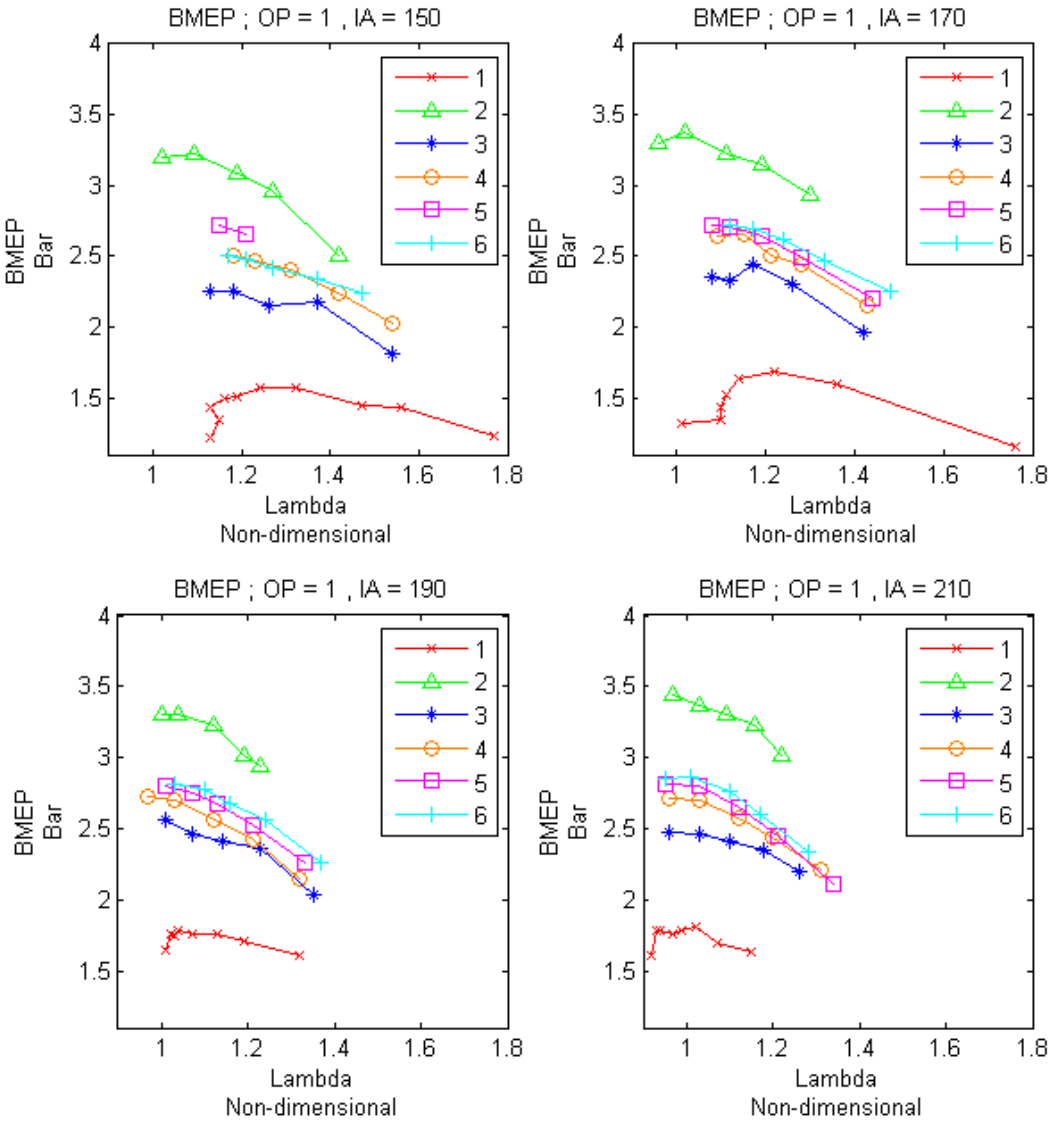

Figure 29: BMEP results for all configurations at operating point one

The power output at operating points one and two are shown in Figure 29 and Figure 30 in terms of BMEP. The trends closely follow those of the other measurements. At point one, an 86% increase in power output with the addition of power valves. The valve-less PR-SCT (configuration three) achieved 39% higher BMEP than configuration one. Increases of 6%,

9%, and 12% compared to configuration three were recorded for configurations four, five, and six respectively. At operating point two, the increase provided by the power valve is lower. A 28% increase is provided by the power valves, configuration three achieves an 8.1% improvement over configuration one, and the PR-SCT achieves a 16% increase over configuration three.

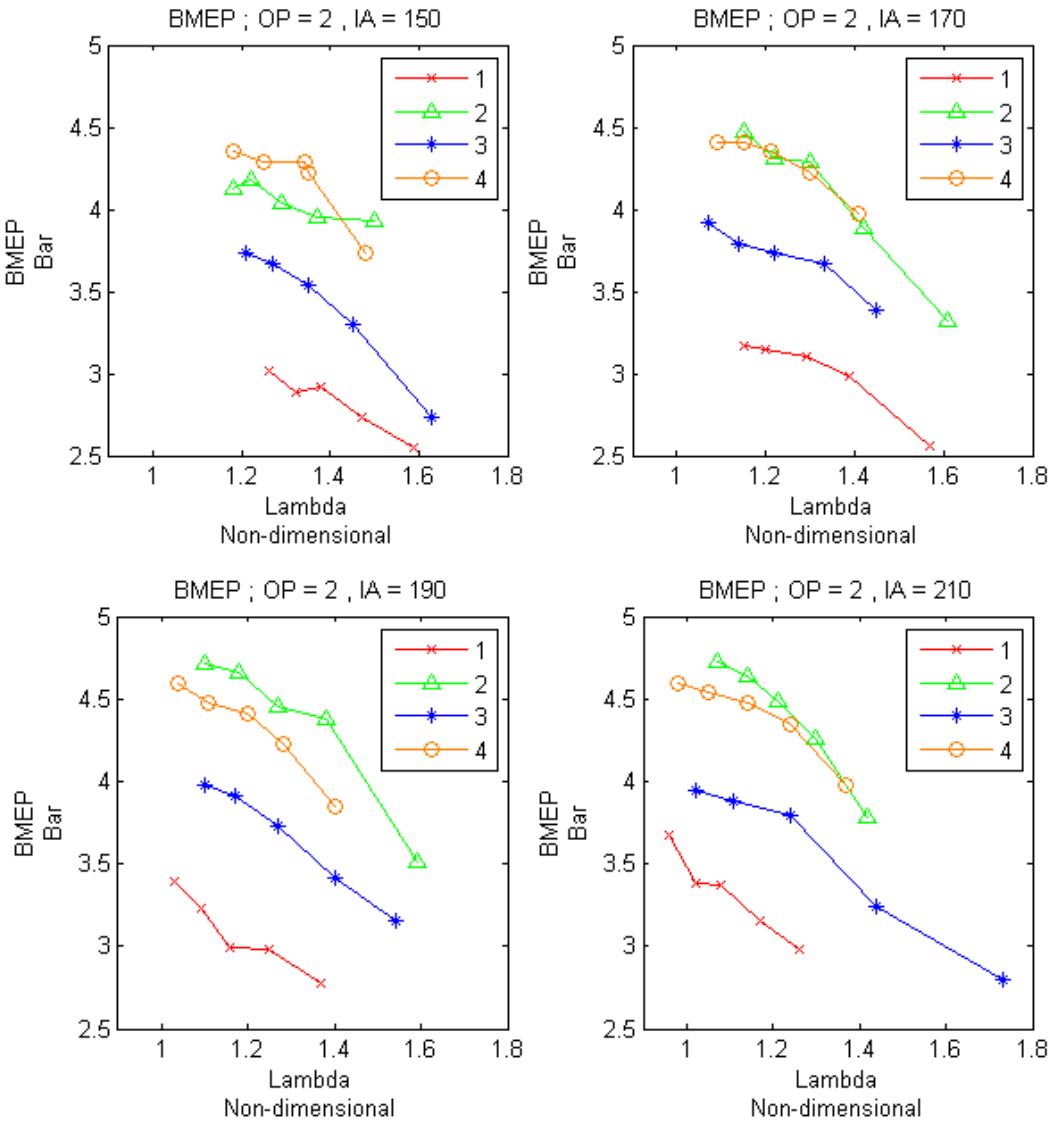

Figure 30: BMEP results for configurations one through four at operating point two

Configuration	BMEP
1	4.9
2	7.6
3	5.4
4	6.0
5	6.4
6	6.2

Table 6: Peak BMEP results for all configurations at operating point three

Configuration	BMEP
1	6.8
2	7.5
3	7.1
4	7.6

Table 7: Peak BMEP results for configurations one through four at operating point four

Increasing BMEP at WOT is desired to improve the performance aspect of the engine. Table 6 shows the BMEP at 5200 RPM and WOT for all six configurations. The output is raised by 55% by lowering the power valves. The addition of the valves in configurations four through six only improves the output by 11%, 18%, and 15% respectively over configuration three. Table 7 shows the BMEP data for operating point four. At the higher speed of 6000 RPM at WOT, the PR-SCT configuration achieves a higher BMEP than the power valve configuration, with an improvement of 7% compared to configuration three. The power valves do produce a greater improvement over the baseline; 10% higher than configuration one.

5.4 Trapping Efficiency

There are multiple methods to measure the trapping efficiency of engines. Most of these methods are indirect, and most have stipulations that a difficult to meet. Easily adaptable methods rely heavily on assumptions of homogeneous charging and/or the combustion process fitting a model. The first method, shown as Equation 10, uses the assumption that

there is no oxygen in the products of combustion [3]. Under very fuel rich combustion, the oxygen level will be low, but not zero [6]. An oxygen concentration after combustion of the trapped charge could be assumed to a particular value to increase the accuracy of the result by his method, but the basis of the value would need to be sound. Another method, shown in Equation 11, uses stoichiometry to account for the atomic oxygen in the exhaust stream [4]. The water gas shift model, Equation 12 and Equation 13, is included in its formulation. This formulation still relies on the assumption that oxygen concentration in the exhaust stream is contributed by short-circuiting only. Another method, Equation 14, is based on the carbon balance rather than oxygen balance [4]. This requires the assumption that the short-circuited charge is of the same AFR as the global AFR. An engine with homogeneous scavenging will comply with this condition. It also requires the assumption that the HC in the exhaust stream is only contributed by the short-circuiting. For a homogeneously charged two-stroke operating near stoichiometric AFR, this will be satisfied.

$$TE_{o_2} = 1 - \frac{1 + AFR}{AFR} * \frac{[O_{2\ measured}]}{[O_{2\ ambiant}]}$$

Equation 10: Trapping efficiency given 0_2 concentration and AFR

$$TE_{air} = \frac{.5 * [CO] + [CO_2] + .25 * \alpha * k_w * ([CO] + [CO_2]) + .5 * [NO]}{[O_2] + .5 * [CO] + [CO_2] + .25 * \alpha * k_w * ([CO] + [CO_2]) + .5 * [NO]}$$

Equation 11: Trapping efficiency based on oxygen balance

Where

$$k_w = \frac{k * [CO_2]}{[CO] + k * [CO_2]}$$

Equation 12: Water gas shift equation

And

$$k = 3.25 - 3.8 \quad (water\ gas\ equilibruim\ constant)$$

Equation 13: Water gas shift equilibrium constant

$$TE_{fuel} = 1 - \frac{[HC]}{[HC] + [CO] + [CO_2]}$$

Equation 14: Trapping efficiency based on carbon balance

In the case of a direct injected two-stroke engine, none of these models are valid. Under early injection and rich operation, the TE_{air} formulation becomes a good approximation for TE. Otherwise, the TE_{air} formulation can be interpreted as fraction of O_2 that is consumed. The TE_{fuel} formulation can always be used to interpret the fraction of fuel completely combusted, which is a valuable tool for other calibration objectives. The unburned fuel fraction ($1\text{-}TE_{fuel}$) is used to compare TE for constant IA. Figure 31and Figure 32 show the unburned fuel fraction at operating points one and two respectively. The factors driving these values are the same as those for HC and BSFC.

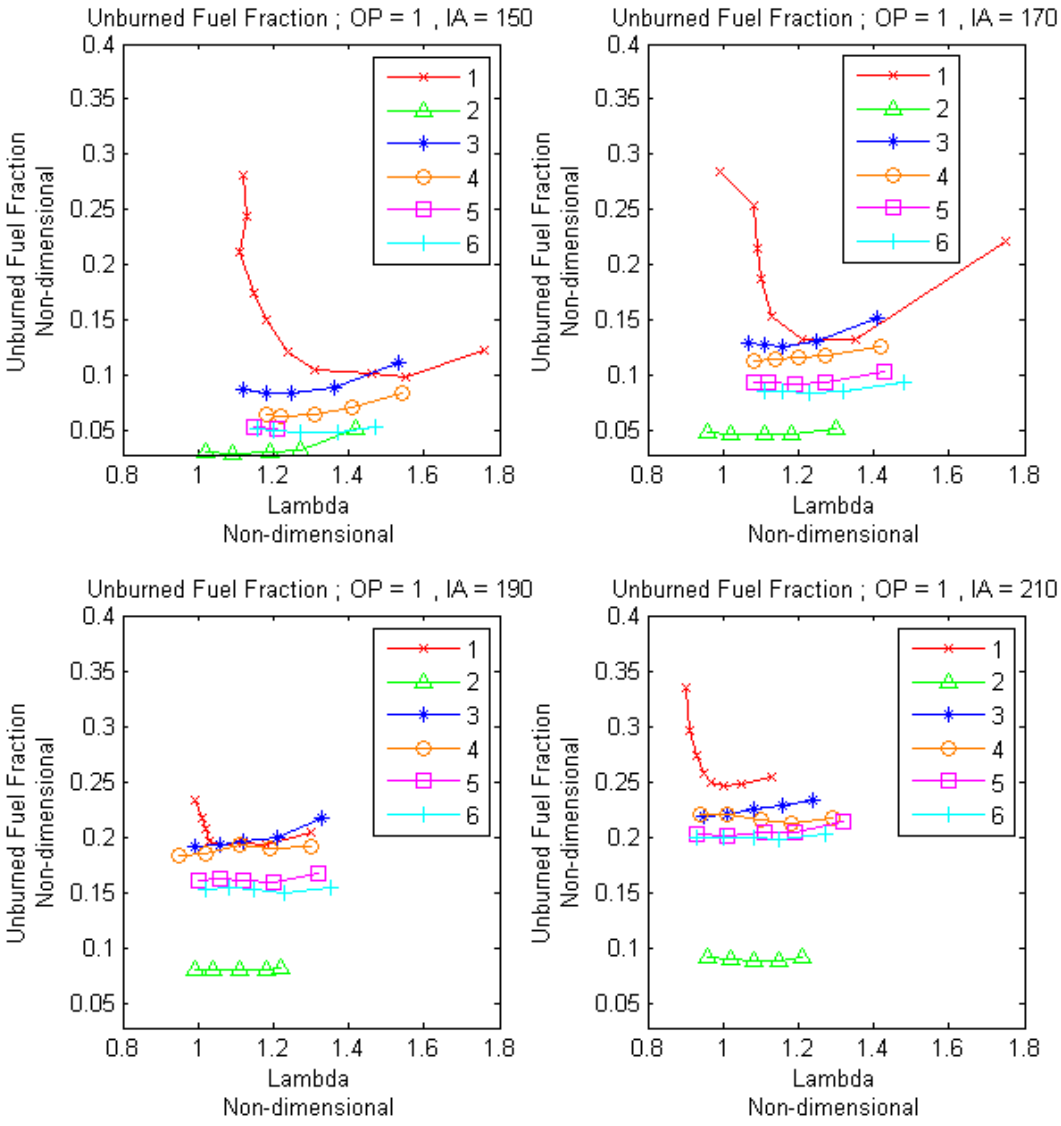

Figure 31: Unburned fuel fraction results for all six configurations operating point one

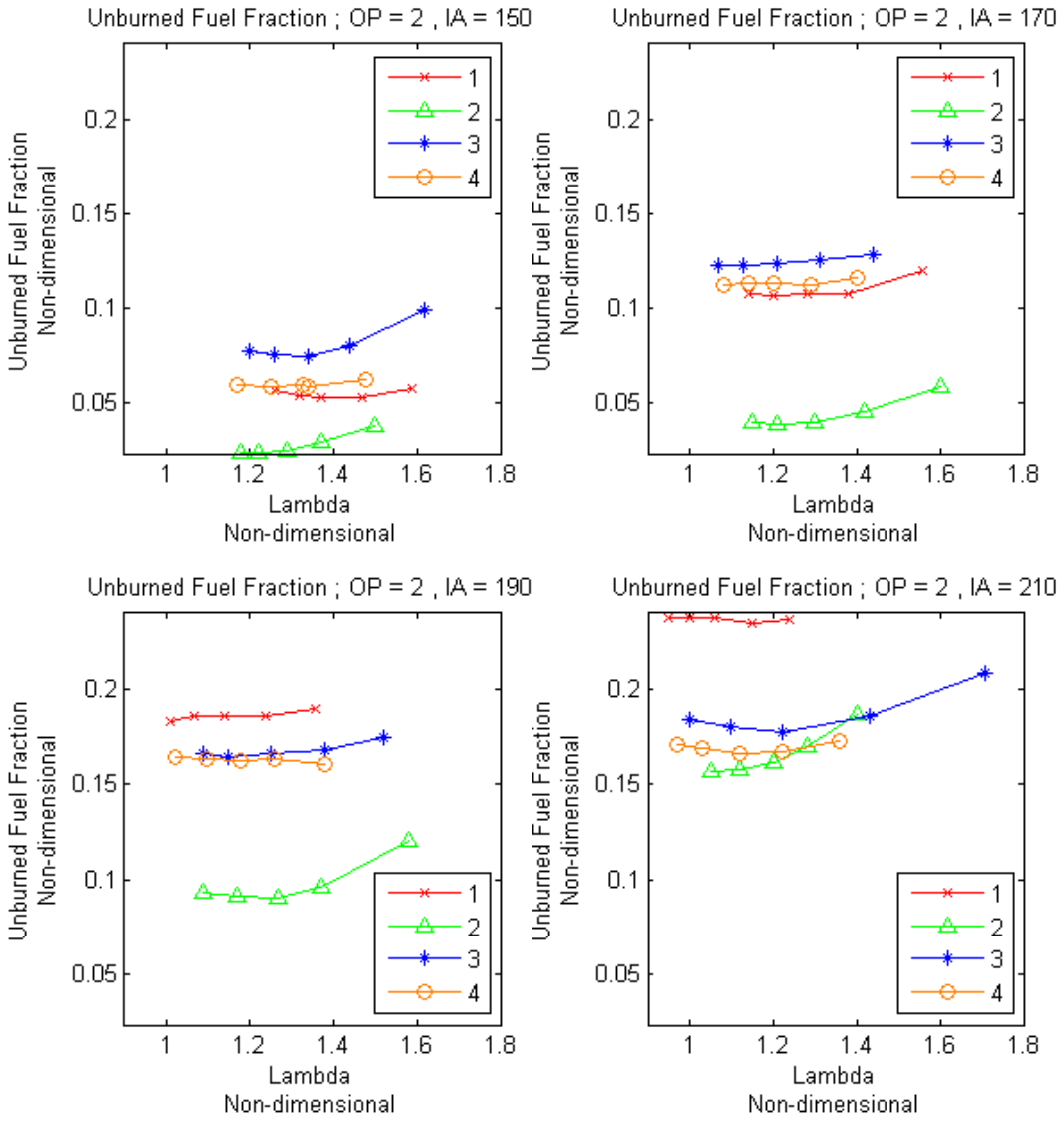

Figure 32: Unburned fuel fraction results for configurations one through four at operating point two

The trapping efficiency calculated by Equation 11 for recorded data samples are shown in Table 8. For operating points one and two, the data used were those of earliest IA and most fuel rich settings. The data show that the power valve produces the highest trapping efficiency at every operating point. At the high speed and high load point, the presence of a power valve does affect the TE as drastically. The PR-SCT shows improvement over

configuration three consistently, with little variation between configurations four through six.

Operating Point	C-1	C-2	C-3	C-4	C-5	C-6
1	69%	84%	73%	75%	76%	76%
2	71%	75%	71%	75%		
3	52%	59%	51%	56%	56%	56%
4	58%	59%	55%	57%		

Table 8: Trapping efficiency results from engine testing

6 Conclusions

6.1 Change in Trapping Efficiency

The TE for each configuration can be compared by analyzing the BMEP and unburned fuel fraction or HC emissions. Although this method is not a direct measure of the TE, a trend of increased BMEP and reduced HC emissions is inherent with increased TE. First, by lowering the power valve (changing from configuration one to configuration two) at operating point one, the BMEP rises dramatically and the HC emissions are also reduced. These features should be examined, particularly under conditions of early injection where the fuel is mixed into the cylinder early in the cycle. Looking at these characteristics at operating point one where the PR-SCT valve is used, it can be noted that the TE appears to improve as the valve angle is retarded.

Looking at operating point two, it can again be seen that the TE is increased as the power valve is closed. The PR-SCT valve also increases the TE, but with less influence than the factory power valve. Although the HC data for operating points three and four are not valid for this comparison, the BMEP data do show a similar trend. The PR-SCT valve performs better at 6000 RPM than at 5200 RPM in relationship to the improvement yielded from the power valve. These conclusions are consistent with the values shown in Table 8.

6.2 Change in SR, SE

The SR cannot be accurately calculated with the collected data. A possible means of calculation is shown in Equation 16. The mass flow rate of fuel ($\dot{m}_{fuel}$) is recorded and the volumetric flow rate of the reference charge ($\dot{V}_{ref}$) are known. The density of the reference charge is a function of ambient air temperature, which was not recorded. The AFR can be

approximated by analysis of the exhaust gases. Two methods were used to calculate the AFR. One method incorporated the creation of NO [4]. The other incorporates the water-gas shift reaction while neglecting the NO component [17]. The water-gas shift reaction is shown in Equation 12. The equilibrium of the reaction relates the production of CO and H_2 in the combustion products. Discrepancies between these two values, along with the lack of air temperature data, led to this approach being discarded.

$$CO + H_2O \Leftrightarrow CO_2 + H_2$$

Equation 15: Water-gas shift reaction

$$SR = \frac{m_{as}}{m_{ref}} = \frac{AFR * \dot{m}_{fuel}}{\dot{V}_{ref} * \rho(T)}$$

Equation 16: Calculation of SR with experimental data

Some speculations and inferences can still be made with the data to find how the hardware configurations compare. As the SE decreases, the concentration of oxygen does also. With the assumption that this will increase CO emissions, and the data from 5.2.2 (especially the chart where IA=190 in Figure 26), a conclusion can be drawn that the SE is higher for the PR-SCT configuration. This hypothesis is not sound; however, as CO emissions can be affected by many other factors. At operating point one, for instance, configuration one produces much higher CO. The culprit for this is much more likely to be the low engine load than a reduced SE.

6.3 Exhaust port seal

One important result is the assessment of the ability for the PR-SCT valve to seal off the exhaust port when it meets the piston. Most of the data support the conclusion that the seal is

very poor. As seen in Table 8, the TE is unaffected by the phase of the exhaust valve. If the valve were sealing the cylinder properly, then the TE would undoubtedly increase with advanced valve phasing.

6.4 Comparison of configuration one and three

The various hardware configurations differ in the time at which the exhaust port closes and/or opens. Configurations one and three have identical exhaust port timings. However, the results from testing are not identical. Configuration three includes more restrictions in the exhaust runner than configuration one. Additionally, during the manufacturing process of the cylinders used in configurations three through six, material was removed from the top and bottom of the cylinder block to provide a flat surface after warping that occurred during welding. As a result, the combustion chamber volume is reduced, and the compression ratio increased. The compression ratio was increased from 12:1 to about 13:1. These two variations can account for this discrepancy in measured results between the configurations.

7 Future Work

7.1 PR-SCT design modifications

As stated in section 6.3, the PR-SCT valve does not seal the cylinder well enough to yield the anticipated TE improvements. To better this seal, the clearance from the valve to the piston face should be reduced. The valve used in this study had a clearance of approximately three millimeters. A suitable clearance for exhaust valves is less than one millimeter [18]. As such the valve should be re-designed and manufactured such that the face is much closer to the piston.

The exhaust flow restriction discussed in 6.4 should be further explored. A flow bench should be used with the two sets of cylinders and varying valve positions to quantify the resistance to fluid flow out the exhaust port. One possible way to improve restriction caused by valve position during blow-down is to re-design the system to incorporate a valve with longer radius and a further shaft offset.

7.2 Trapping Efficiency testing procedures

If measuring the TE is a goal for testing, and a DI system is used, then an early injection and fuel rich operation should be used. Using a constant IA between testing configurations will further simplify this process. Using a moderately high CO concentration will ensure the highest O_2 consumption during combustion. This will lead to the highest accuracy. To increase repeatability of this experiment a two-part approach can be used. The first step is holding the CO at 3% concentration to make an initial TE assessment. With an initial TE value and Equation 17**,** an objective of CO concentration in the combustion gases can be

made. From the results of this testing 4% CO concentration of the combusted charge was found to be a satisfactory objective.

$$[CO]_{combustion} = TE * [CO]_{exhaust\ stream}$$

Equation 17: CO concentration of the combusted charge

Alternatively, for quantifying charging flows through the engine, a more rudimentary fueling system is beneficial. A throttle body injection system or even a carburetor will allow the homogeneous charge assumption to hold true, allowing for the use of unburned fuel fraction as an avenue to calculate TE. This will also simplify the testing procedure by completely eliminating one of the variables, IA.

7.3 Data collection

To increase the value of future engine studies at the University of Idaho, additional measurement tools should be used. These tools will provide insight into metrics more suitable for comparisons of this caliber.

7.3.1 Crank encoder

A crank encoder with high resolution is necessary to operate the combustion analyzer [19]. The utility of this type of analyzer is un-paralleled in the internal combustion engine industry. One of its core functions is calculating the Indicated Mean Effective Pressure (IMEP). The IMEP is a metric of the work done onto the piston by the cylinder charge. It differs from the BMEP only by the work consumed by friction within the engine. IMEP is a more direct approach to relate engine output performance. Coefficient of Variance (COV) of the IMEP is another tool, which allows a researcher to quantify cycle-to-cycle variations.

7.3.2 Water-cooled pressure transducer

In addition to the crank encoder, a water-cooled pressure transducer can be deployed near the exhaust port. This sensor would be able to show pressure trends in the cylinder during the scavenging process, like the ones in Figure 12, Figure 13, and Figure 14. For this, the in-cylinder transducer used for the combustion analyzer is not sensitive enough to determine the effect of the PR-SCT valve.

7.3.3 Standardize testing preparation

In an effort to produce meaningful values the data collection equipment should be properly prepared before each round of testing. The Horiba emissions analyzer should be programmed for the proper fuel and have the HC hang-up procedure performed daily to improve accuracy. Additionally, the filters should be replaced and a leak test performed on the onset of daily operation.

Although it is understood that the value is inaccurate, to improve consistency of the Innovate LM-2 Air/Fuel Ratio Meter, it should have the proper fuel composition entered into the unit. As is the case in this data set, the dynamometer was not calibrated properly. The slope need not be calibrated regularly, but the zero mark should be set whenever testing is initiated. The zero should be set when the dynamometer coolant water is flowing, as it impacts the load on the head.

7.4 Fuel temperature regulation

The University of Idaho Clean Snowmobile Challenge team (UICSC) has designed with emphasis on elegant solutions to the needs of the competition since their first competition in 2001. One possible design feature for upcoming years could be fuel conditioning. The

system in place uses fuel at source temperature for injection and cooling of the injectors and EMM. Fuel temperature plays an important role in charge cooling as well as evaporation and heat release rates. Conditioning the fuel temperature can change an uncontrolled variable to a constant, or allow control for optimization.

When high performance is the goal, cold fuel is desired. This cold fuel reduces temperatures in the cylinder during scavenging and compression, thus allowing higher charge densities and detonation deterrence. At low loads, especially with direct injection, the cold fuel does not evaporate as readily as a fuel injected at higher temperature. This can result in faster heat release during combustion, which can improve thermal efficiency, and lower emissions of CO and HC. In addition, the fuel can be introduced to the cylinder later in the cycle, leading to less short-circuited fuel mixture without penalties of an increase in HC and CO.

A simple counter-flow heat exchanger can be utilized to bring injection fuel up to the same temperature as the engine coolant. Snowmobile cooling systems are designed to regulate the cooling temperature above 37°C (99 °F) [20], a temperature that the injection hardware will easily withstand. An electronic solenoid can be used to divert flow of either of the fluids away from the heat exchanger, thus allowing low temperature fuel for high performance operation. The proposed system would provide the potential for increased fuel economy without a reduction in power output or significant added complexity.

Bibliography

[1] G. A. Florides and P. Christodoulides, "Global Warming and Carbon Dioxide Through Sciences," *Environment International,* vol. 35, pp. 390-401, 2009.

[2] A. Welch, Performance and Emissions Analysis of a Synchronous Charge Trapped Two-Stroke Engine, Moscow: Master's Thesis, 2012.

[3] G. p. Blair, Design and Simulation of Two-Stroke Engines, Warrendale, PA: Society of Automotive Engineers, 1996.

[4] N. Bradbury, Retrofitting Direct-Injection and a Turbocharger to a Two-Stroke Engine for Snowmobile Application, Moscow: Master's Thesis, 2006.

[5] J. B. Heywood and E. Sher, The Two Stroke Cycle Engine, Philadelphia: Taylor & Francis, 1999.

[6] R. Stone, Introduction to Internal Combustion Engines, Chippenham: Macmillan Press, 1999.

[7] M. Nuti, Emissions from Two-Stroke Engines, Warrendale: Society of Automotive Engineers, 1998.

[8] R. D. Zucker and O. Biblarz, Fundamentals of gas dynamics, Hoboken: John Wiley & Sons, 2002.

[9] Lotus Engineering, "Could upsizing be the new downsizing," *proActive,* pp. 24-27, Feb

2010.

[10] Group Lotus PLC, "Omnivore Interactive Animation," Group Lotus PLC, 2013. [Online]. Available: http://www.lotuscars.com/us/omnivore-interactive-animation. [Accessed 20 June 2013].

[11] P. Britanyak, Synchronous Charge Trapping Modification of a Two-Stroke Engine, Moscow: Master's Thesis, 2010.

[12] A. Hooper, A. Fuhrman, C. Bode and T. Lord, "Rotary Synchronous Charge Trapping". United States of America Patent WO2012161800 A2, 29 November 2012.

[13] F. Alex, A. Hooper, L. Ty and B. Coleman, "Synchronous Charge Trapping Final Report", Moscow: Not yet published, 2011.

[14] D. Dixon, Comparison of Variable Exhaust Flow Techniques in a Modern Two-Stroke Engine, Moscow: Master's Thesis, 2012.

[15] C. C. Lela and J. J. White, "Laboratory Testing of Snowmobile Emissions," Southwest Research Institute, San Antonio, 2002.

[16] S. R. Turns, An Introduction to Combustion, New York: McGraw-Hill, 2012.

[17] Horiba, Automotive Emissions Analyzer MEXA-584L Instruction Manual, Kyoto: Horiba Ltd., 2008.

[18] J. Johnson, Interviewee, *Personal Correspondence.* [Interview]. July 2011.

[19] Hi-Techniques, REVelation Operators Manual, Madison, 2004.

[20] Bombardier Recreational Products, Ski-doo 2009 shop manual, Valcourt: Bombardier Recreational Products Technical Publications, 2008.

[21] J. Johnson, Comparison of Stratified and Homogeneous Combustion in a Direct-injected Two-stroke Engine for Snowmobile Applications, Moscow: Master's Thesis, 2007.

Appendices

Appendix A: Collected Data

Comments	Configuration	Test Point	Angle #	Run #	RPM	Throttle Counts	Injection Angle	Injection Quantity	Power (HP)	λ (LM-2)	Fuel Flow (kg/hr)	EGT	Emissions					
													CO (%)	CO_2 (%)	HC PPM	NO_X PPM	λ	O_2 (%)
	1	1	1	1	5200	100	150	6.0	8.6	1.8	2.40	770	0.53	6.86	1622	-22	1.77	11.20
	1	1	1	2	5200	100	150	6.5	10.0	1.63	2.52	770	0.84	7.79	1466	-22	1.56	9.69
	1	1	1	3	5200	100	150	7.0	10.1	1.45	2.76	800	1.21	8.12	1632	45	1.47	9.29
	1	1	1	4	5200	100	150	7.6	11.0	1.26	3.00	800	2.29	8.05	1860	42	1.32	8.48
	1	1	1	5	5200	100	150	8.1	11.0	1.16	3.48	790	3.05	7.65	2257	46	1.24	8.39
	1	1	1	6	5200	100	150	8.7	10.5	1.11	3.60	765	3.65	7.14	2945	54	1.19	8.60
	1	1	1	7	5200	100	150	9.3	10.4	1.06	3.84	755	3.99	6.76	3512	61	1.16	8.84
	1	1	1	8	5200	100	150	9.9	10.0	1.04	4.08	735	4.24	6.31	4365	70	1.13	9.27
	1	1	1	9	5200	100	150	10.4	9.4	1.02	4.44	715	4.26	5.63	4982	74	1.15	10.21
	1	1	1	10	5200	100	150	11.0	8.5	1.00	4.68	680	4.41	5.05	5802	78	1.13	10.80
	1	1	2	1	5200	100	160	6.0	9.1	1.73	2.52	730	0.48	7.38	1913	-20	1.65	10.55
	1	1	2	2	5200	100	160	6.6	11.0	1.41	2.88	815	1.15	8.36	1767	-21	1.41	8.69
	1	1	2	3	5200	100	160	7.1	11.3	1.28	3.24	830	2.09	8.18	1954	-20	1.30	8.14
	1	1	2	4	5200	100	160	7.7	11.4	1.15	3.48	810	3.19	7.56	2413	-17	1.21	8.06
	1	1	2	5	5200	100	160	8.3	10.8	1.09	3.84	780	3.88	6.87	3208	-10	1.16	8.44
	1	1	2	6	5200	100	160	8.9	10.3	1.05	3.84	755	4.17	6.39	3815	-2	1.14	8.84
	1	1	2	7	5200	100	160	9.4	10.2	1.03	4.20	740	4.25	5.98	4337	2	1.13	9.33

Comments	Configuration	Test Point	Angle #	Run #	RPM	Throttle Counts	Injection Angle	Injection Quantity	Power (HP)	λ (LM-2)	Fuel Flow (kg/hr)	EGT	Emissions					
													CO (%)	CO_2 (%)	HC PPM	NO_x PPM	λ	O_2 (%)
	1	1	2	8	5200	100	160	10.0	9.9	1	4.44	725	4.43	5.41	5021	5	1.13	9.96
	1	1	3	1	5200	100	170	6.0	8.1	1.9	2.28	660	0.31	6.28	2944	-5	1.76	12.18
	1	1	3	2	5200	100	170	6.7	11.1	1.4	2.88	830	1.00	8.58	2259	-12	1.36	8.51
	1	1	3	3	5200	100	170	7.4	11.8	1.21	3.24	830	2.50	8.22	2502	-15	1.22	7.75
	1	1	3	4	5200	100	170	8.1	11.4	1.08	3.60	800	3.77	7.28	3094	-11	1.14	7.97
	1	1	3	5	5200	100	170	8.9	10.6	1.04	3.96	765	4.30	6.53	3847	-6	1.11	8.54
	1	1	3	6	5200	100	170	9.6	10.0	1	4.20	750	4.59	5.93	4481	-1	1.10	9.11
	1	1	3	7	5200	100	170	10.3	9.4	0.98	4.32	710	4.77	5.21	5281	3	1.10	9.90
	1	1	3	8	5200	100	170	11.0	9.2	0.96	4.80	680	5.25	5.12	6402	20	1.01	9.58
	1	1	4	1	5200	100	180	7.0	10.2	1.5	3.00	800	0.74	8.52	2590	29	1.39	8.92
	1	1	4	2	5200	100	180	7.4	11.2	1.21	3.00	852	1.82	8.83	2860	49	1.22	7.75
	1	1	4	3	5200	100	180	7.9	11.1	1.1	3.48	836	3.20	8.13	3177	54	1.13	7.57
	1	1	4	4	5200	100	180	8.3	11.8	1.05	3.60	810	3.97	7.45	3641	59	1.10	7.86
	1	1	4	5	5200	100	180	8.7	10.9	1.01	3.72	787	4.41	6.96	4153	63	1.07	8.15
	1	1	4	6	5200	100	180	9.1	10.6	0.99	3.84	774	4.63	6.68	4639	69	1.05	8.37
	1	1	4	7	5200	100	180	9.6	11.5	0.99	3.84	786	4.52	6.59	4333	27	1.07	8.33
	1	1	4	8	5200	100	180	10.0	11.1	0.97	4.20	771	4.84	6.20	4938	40	1.04	8.61
	1	1	5	1	5200	100	190	7.5	11.2	1.4	3.12	814	0.75	8.40	3644	50	1.32	9.02
	1	1	5	2	5200	100	190	7.9	11.9	1.22	3.48	860	1.40	8.89	3778	48	1.19	7.83
	1	1	5	3	5200	100	190	8.2	12.3	1.13	3.48	870	2.06	8.77	3988	48	1.13	7.44
	1	1	5	4	5200	100	190	8.6	12.3	1.05	3.72	855	3.23	8.14	4180	48	1.07	7.29
	1	1	5	5	5200	100	190	8.9	12.4	1.02	3.84	843	3.82	7.72	4333	50	1.04	7.37
	1	1	5	6	5200	100	190	9.3	12.2	1	3.96	832	4.22	7.29	4611	52	1.03	7.61
	1	1	5	7	5200	100	190	9.6	12.3	0.99	3.96	818	4.44	7.02	4881	56	1.02	7.80
	1	1	5	8	5200	100	190	10.0	11.5	0.9	4.20	800	4.67	6.68	5317	59	1.01	8.08
	1	1	6	1	5200	100	200	8.0	11.5	1.3	3.36	823	0.78	8.69	4390	66	1.24	8.62
	1	1	6	2	5200	100	200	8.4	12.1	1.18	3.36	868	1.49	9.09	4643	61	1.12	7.50
	1	1	6	3	5200	100	200	8.9	12.9	1.05	3.84	865	2.89	8.53	4900	58	1.04	7.12

Comments	Configuration	Test Point	Angle #	Run #	RPM	Throttle Counts	Injection Angle	Injection Quantity	Power (HP)	λ (LM-2)	Fuel Flow (kg/hr)	EGT	Emissions					
													CO (%)	CO_2 (%)	HC PPM	NO_x PPM	λ	O_2 (%)
	1	1	6	4	5200	100	200	9.3	12.6	1.02	4.08	853	3.54	8.06	5043	58	1.02	7.21
	1	1	6	5	5200	100	200	9.7	12.5	0.97	4.20	844	4.04	7.55	5378	60	1.00	7.47
	1	1	6	6	5200	100	200	10.1	12.1	0.97	4.32	826	4.42	7.07	5849	63	0.98	7.80
	1	1	6	7	5200	100	200	10.6	11.8	0.95	4.56	798	4.74	6.54	6576	67	0.96	8.25
	1	1	6	8	5200	100	200	11.0	12.0	0.96	4.68	768	4.71	6.26	7384	74	0.95	8.66
	1	1	7	1	5200	100	210	8.3	11.4	1.23	3.60	833	1.05	8.91	5194	72	1.15	8.13
	1	1	7	2	5200	100	210	8.8	11.8	1.11	3.72	865	1.74	9.10	5448	66	1.07	7.34
	1	1	7	3	5200	100	210	9.2	12.6	1.05	4.08	868	2.57	8.77	5671	64	1.02	7.09
	1	1	7	4	5200	100	210	9.7	12.4	1.01	4.08	861	3.27	8.29	5888	63	0.99	7.15
	1	1	7	5	5200	100	210	10.1	12.3	0.99	4.20	853	3.78	7.85	6143	64	0.97	7.31
	1	1	7	6	5200	100	210	10.6	12.4	0.96	4.44	826	4.34	7.24	6704	66	0.94	7.66
	1	1	7	7	5200	100	210	11.0	12.4	0.95	4.68	812	4.50	6.85	7347	71	0.93	8.06
	1	1	7	8	5200	100	210	11.5	11.2	0.96	4.68	780	4.45	6.44	8448	81	0.92	8.67
	1	1	8	1	5200	100	220	8.3	11.0	1.35	3.48	807	0.39	8.51	5315	74	1.24	9.18
	1	1	8	2	5200	100	220	8.8	12.0	1.2	3.36	858	0.83	9.33	5456	68	1.12	7.77
	1	1	8	3	5200	100	220	9.2	12.0	1.11	3.60	873	1.62	9.33	5762	65	1.05	7.16
	1	1	8	4	5200	100	220	9.7	12.3	1.05	4.08	870	2.59	8.90	5921	62	1.00	6.94
	1	1	8	5	5200	100	220	10.1	12.2	1	4.08	862	3.25	8.51	6085	61	0.97	6.90
	1	1	8	6	5200	100	220	10.6	12.4	0.98	4.44	840	4.18	7.75	6507	61	0.94	7.14
	1	1	8	7	5200	100	220	11.0	12.4	0.1	4.56	822	4.57	7.34	6935	64	0.92	7.39
	1	1	8	8	5200	100	220	11.5	11.4	0.09	4.80	804	4.62	6.91	7762	69	0.91	7.95
	2	1	1	1	5200	100	150	7.5	17.5	1.44	3.12	1007	0.28	9.83	861	133	1.42	7.53
	2	1	1	2	5200	100	150	8.3	20.6	1.26	3.36	1012	0.64	11.01	590	222	1.27	5.71
	2	1	1	3	5200	100	150	9.0	21.5	1.18	3.72	1017	1.17	11.31	603	248	1.19	4.86
	2	1	1	4	5200	100	150	9.8	22.5	1.06	4.32	1000	2.63	10.93	623	203	1.09	4.22
	2	1	1	5	5200	100	150	10.5	22.3	0.99	4.44	974	4.22	10.13	685	158	1.02	3.98
	2	1	2	1	5200	100	170	8.3	20.5	1.3	3.36	995	0.30	10.86	921	237	1.30	6.16
	2	1	2	2	5200	100	170	9.1	22.0	1.19	3.84	985	0.71	11.63	930	286	1.19	4.83

Comments	Configuration	Test Point	Angle #	Run #	RPM	Throttle Counts	Injection Angle	Injection Quantity	Power (HP)	λ (LM-2)	Fuel Flow (kg/hr)	EGT	Emissions					
													CO (%)	CO_2 (%)	HC PPM	NO_x PPM	λ	O_2 (%)
	2	1	2	3	5200	100	170	9.8	22.5	1.09	4.08	980	1.68	11.55	973	274	1.11	4.20
	2	1	2	4	5200	100	170	10.6	23.5	0.99	4.56	978	3.58	10.63	1077	195	1.02	3.86
	2	1	2	5	5200	100	170	11.3	23.0	0.93	5.04	956	5.20	9.73	1162	137	0.96	3.72
	2	1	3	1	5200	100	190	9.0	20.5	1.25	3.84	980	0.17	11.32	1573	300	1.23	5.70
	2	1	3	2	5200	100	190	9.5	21.0	1.21	4.20	990	0.26	11.71	1604	335	1.19	5.12
	2	1	3	3	5200	100	190	10.0	22.5	1.13	4.32	1005	0.72	12.06	1674	359	1.12	4.31
	2	1	3	4	5200	100	190	10.5	23.0	1.02	4.68	1000	1.93	11.74	1783	301	1.04	3.81
	2	1	3	5	5200	100	190	11.0	23.0	0.99	4.68	988	3.15	11.08	1868	229	1.00	3.66
	2	1	4	1	5200	100	210	9.0	21.0	1.25	3.72	955	0.09	11.38	1751	313	1.22	5.67
	2	1	4	2	5200	100	210	9.6	22.5	1.17	4.20	975	0.17	12.02	1776	400	1.16	4.78
	2	1	4	3	5200	100	210	10.3	23.0	1.1	4.44	1000	0.74	12.32	1909	413	1.09	3.97
	2	1	4	4	5200	100	210	10.9	23.5	1.04	4.44	1005	1.80	11.93	2057	328	1.03	3.66
	2	1	4	5	5200	100	210	11.5	24.0	0.97	5.28	990	3.37	11.09	2186	213	0.97	3.52
	3	1	1	1	5200	100	150	7.0	12.6	1.65	2.76	910	0.49	8.25	1695	31	1.54	9.51
	3	1	1	2	5200	100	150	7.5	15.2	1.4	3.12	957	1.13	8.96	1531	33	1.37	8.07
	3	1	1	3	5200	100	150	8.0	15.0	1.24	3.24	952	2.13	8.89	1549	34	1.26	7.33
	3	1	1	4	5200	100	150	8.5	15.7	1.13	3.60	940	3.14	8.53	1658	36	1.18	6.97
	3	1	1	5	5200	100	150	9.0	15.7	1.06	3.72	930	3.94	8.17	1785	39	1.13	6.79
	3	1	2	1	5200	100	170	7.5	13.7	1.37	3.24	941	0.30	8.81	2529	46	1.42	9.00
	3	1	2	2	5200	100	170	8.0	16.1	1.3	3.48	972	0.85	9.69	2434	49	1.26	7.38
	3	1	2	3	5200	100	170	8.5	17.0	1.17	3.84	961	2.00	9.42	2517	43	1.17	6.80
	3	1	2	4	5200	100	170	9.0	16.2	1.11	3.84	953	2.84	9.06	2644	40	1.12	6.55
	3	1	2	5	5200	100	170	9.5	16.4	1.05	3.96	938	3.57	8.68	2768	39	1.08	6.42
	3	1	3	1	5200	100	190	8.0	14.2	1.44	3.48	930	0.22	8.63	3786	50	1.35	9.21
	3	1	3	2	5200	100	190	8.6	16.5	1.3	3.60	967	0.33	9.69	3844	58	1.23	7.71
	3	1	3	3	5200	100	190	9.3	16.8	1.21	3.96	982	0.85	10.05	4042	63	1.14	6.87
	3	1	3	4	5200	100	190	9.9	17.2	1.11	4.20	975	1.75	9.87	4238	60	1.07	6.39
	3	1	3	5	5200	100	190	10.5	17.9	1.02	4.80	955	3.02	9.28	4438	53	1.01	6.14

Comments	Configuration	Test Point	Angle #	Run #	RPM	Throttle Counts	Injection Angle	Injection Quantity	Power (HP)	λ (LM-2)	Fuel Flow (kg/hr)	EGT	Emissions					
													CO (%)	CO_2 (%)	HC PPM	NO_x PPM	λ	O_2 (%)
	3	1	4	1	5200	100	210	9.0	15.3	1.37	3.60	933	0.15	9.15	4361	61	1.26	8.58
	3	1	4	2	5200	100	210	9.6	16.4	1.25	3.96	969	0.27	9.83	4555	70	1.18	7.60
	3	1	4	3	5200	100	210	10.3	16.8	1.18	4.32	986	0.74	10.18	4826	76	1.10	6.81
	3	1	4	4	5200	100	210	10.9	17.2	1.07	4.56	974	1.78	10.04	5077	70	1.03	6.21
	3	1	4	5	5200	100	210	11.5	17.3	0.99	4.68	958	3.12	9.45	5322	59	0.96	5.95
	4	1	1	1	5200	100	150	7.0	14.1	1.6	2.76	780	0.34	8.61	1264	55	1.54	9.11
	4	1	1	2	5200	100	150	7.5	15.6	1.43	3.12	815	0.64	9.29	1161	63	1.42	7.98
	4	1	1	3	5200	100	150	8.0	16.8	1.3	3.36	815	1.42	9.42	1152	67	1.31	7.21
	4	1	1	4	5200	100	150	8.5	17.2	1.19	3.60	805	2.36	9.19	1207	66	1.23	6.73
	4	1	1	5	5200	100	150	9.0	17.5	1.13	3.72	800	2.98	8.99	1263	66	1.18	6.47
	4	1	2	1	5200	100	170	7.5	15.0	1.48	3.24	782	0.22	9.07	2064	79	1.43	8.66
	4	1	2	2	5200	100	170	8.1	17.0	1.31	3.60	824	0.51	10.10	2159	106	1.28	7.08
	4	1	2	3	5200	100	170	8.6	17.5	1.22	3.72	832	1.09	10.18	2251	108	1.21	6.55
	4	1	2	4	5200	100	170	9.2	18.5	1.17	3.96	830	1.74	10.06	2306	106	1.15	6.19
	4	1	2	5	5200	100	170	9.7	18.4	1.07	4.08	815	2.93	9.53	2400	89	1.09	5.93
	4	1	3	1	5200	100	190	8.0	15.0	1.4	3.72	770	0.19	9.20	3435	88	1.32	8.55
	4	1	3	2	5200	100	190	8.8	16.9	1.28	3.84	795	0.27	10.11	3714	121	1.21	7.31
	4	1	3	3	5200	100	190	9.5	17.9	1.18	4.08	820	0.67	10.51	4042	143	1.12	6.50
	4	1	3	4	5200	100	190	10.3	18.8	1.1	4.44	825	2.06	10.23	4204	134	1.03	5.78
	4	1	3	5	5200	100	190	11.0	19.0	1	5.04	820	3.51	9.50	4429	112	0.97	5.56
	4	1	4	1	5200	100	210	8.5	15.4	1.41	3.72	760	0.11	8.83	3816	25	1.31	8.56
	4	1	4	2	5200	100	210	9.3	17.0	1.28	4.32	790	0.10	9.79	4102	58	1.20	7.35
	4	1	4	3	5200	100	210	10.0	18.0	1.2	4.44	805	0.23	10.43	4464	96	1.12	6.41
	4	1	4	4	5200	100	210	10.8	18.8	1.08	4.56	822	1.08	10.54	4957	94	1.03	5.66
	4	1	4	5	5200	100	210	11.5	18.9	1.01	4.92	810	2.43	9.95	5298	74	0.96	5.37
Engine still warming up	5	1	1	1	5200	100	150	7.5	15.4	1.5	3.00	830	0.40	8.71	995	56	1.54	8.84
Engine still	5	1	1	2	5200	100	150	8.1	17.0	1.36	3.36	852	1.06	9.26	905	67	1.38	7.57

Comments	Configuration	Test Point	Angle #	Run #	RPM	Throttle Counts	Injection Angle	Injection Quantity	Power (HP)	λ (LM-2)	Fuel Flow (kg/hr)	EGT	Emissions					
													CO (%)	CO_2 (%)	HC PPM	NO_x PPM	λ	O_2 (%)
warming up																		
Engine still warming up	5	1	1	3	5200	100	150	8.6	17.7	1.22	3.84	850	2.00	9.14	940	65	1.28	6.96
	5	1	1	4	5200	100	150	9.2	18.5	1.15	3.84	845	2.78	8.91	988	62	1.21	6.60
	5	1	1	5	5200	100	150	9.7	19.0	1.08	3.96	835	3.67	8.56	1061	57	1.15	6.35
	5	1	2	1	5200	100	170	7.5	15.4	1.45	2.88	810	0.21	9.23	1675	54	1.44	8.32
	5	1	2	2	5200	100	170	8.1	17.4	1.3	3.36	850	0.69	10.10	1710	75	1.28	6.78
	5	1	2	3	5200	100	170	8.6	18.4	1.19	3.48	847	1.52	10.05	1803	74	1.19	6.19
	5	1	2	4	5200	100	170	9.2	18.9	1.09	3.84	837	2.62	9.62	1922	64	1.12	5.86
	5	1	2	5	5200	100	170	9.7	19.0	1.04	3.96	832	3.36	9.28	1989	58	1.08	5.71
	5	1	3	1	5200	100	190	8.0	15.8	1.4	3.36	805	0.17	9.34	2955	61	1.33	8.26
	5	1	3	2	5200	100	190	8.6	17.6	1.26	3.60	840	0.34	10.32	3075	93	1.21	6.80
	5	1	3	3	5200	100	190	9.3	18.7	1.14	3.84	853	0.87	10.58	3323	109	1.13	6.09
	5	1	3	4	5200	100	190	9.9	19.2	1.08	3.96	853	1.72	10.34	3525	104	1.07	5.72
	5	1	3	5	5200	100	190	10.5	19.5	1	4.32	837	2.91	9.79	3666	87	1.01	5.50
	5	1	4	1	5200	100	210	8.5	14.7	1.4	3.24	775	0.12	8.85	3774	65	1.34	8.98
	5	1	4	2	5200	100	210	9.3	17.1	1.27	3.60	817	0.13	10.00	3994	93	1.21	7.42
	5	1	4	3	5200	100	210	10.1	18.5	1.18	3.96	840	0.29	10.66	4258	130	1.12	6.42
	5	1	4	4	5200	100	210	10.9	19.5	1.07	4.32	852	1.34	10.67	4588	126	1.03	5.64
	5	1	4	5	5200	100	210	11.7	19.6	0.97	4.80	837	3.10	9.84	4969	94	0.95	5.30
	6	1	1	1	5200	100	150	7.5	15.6	1.45	3.00	835	0.63	8.91	832	31	1.47	8.14
	6	1	1	2	5200	100	150	7.9	16.3	1.34	3.24	845	1.13	9.17	818	35	1.37	7.39
	6	1	1	3	5200	100	150	8.4	16.9	1.22	3.36	845	2.04	9.07	871	34	1.27	6.76
	6	1	1	4	5200	100	150	8.8	17.3	1.14	3.48	835	2.86	8.80	938	31	1.21	6.43
	6	1	1	5	5200	100	150	9.2	17.5	1.1	3.96	830	3.38	8.62	999	30	1.17	6.25
	6	1	2	1	5200	100	170	7.5	15.7	1.49	3.00	825	0.21	8.86	1453	36	1.48	8.49
	6	1	2	2	5200	100	170	8.0	17.2	1.35	3.24	852	0.55	9.72	1465	59	1.33	7.06
	6	1	2	3	5200	100	170	8.5	18.3	1.21	3.60	865	1.27	9.82	1558	62	1.24	6.39

Comments	Configuration	Test Point	Angle #	Run #	RPM	Throttle Counts	Injection Angle	Injection Quantity	Power (HP)	λ (LM-2)	Fuel Flow (kg/hr)	EGT	Emissions					
													CO (%)	CO_2 (%)	HC PPM	NO_x PPM	λ	O_2 (%)
	6	1	2	4	5200	100	170	9.0	18.8	1.13	3.84	856	2.16	9.58	1670	55	1.17	6.01
	6	1	2	5	5200	100	170	9.5	19.0	1.09	3.96	847	2.88	9.28	1741	47	1.12	5.79
	6	1	3	1	5200	100	190	8.0	15.8	1.41	3.24	822	0.15	9.09	2607	34	1.37	8.23
	6	1	3	2	5200	100	190	8.6	17.9	1.28	3.48	855	0.31	10.00	2759	68	1.24	6.92
	6	1	3	3	5200	100	190	9.3	18.7	1.18	4.08	870	0.68	10.39	3027	95	1.16	6.13
	6	1	3	4	5200	100	190	9.9	19.4	1.11	4.20	870	1.39	10.30	3237	100	1.10	5.71
	6	1	3	5	5200	100	190	10.5	19.6	1.04	4.44	855	2.71	9.70	3402	80	1.03	5.42
	6	1	4	1	5200	100	210	9.0	16.3	1.36	3.72	817	0.11	9.23	3646	47	1.28	8.10
	6	1	4	2	5200	100	210	9.8	18.1	1.24	3.96	845	0.19	10.14	3888	94	1.17	6.77
	6	1	4	3	5200	100	210	10.5	19.3	1.15	4.44	866	0.50	10.58	4202	125	1.10	6.04
	6	1	4	4	5200	100	210	11.3	20.0	1.05	4.68	860	1.73	10.35	4543	116	1.01	5.43
	6	1	4	5	5200	100	210	12.0	19.9	0.98	5.16	845	3.09	9.69	4807	89	0.95	5.18
	1	2	1	1	6000	200	150	9.0	20.5	1.58	4.56		0.97	7.89	840	148	1.59	9.47
	1	2	1	2	6000	200	150	9.6	22.0	1.43	4.80		1.52	8.07	823	165	1.47	8.73
	1	2	1	3	6000	200	150	10.3	23.5	1.28	5.16		2.22	8.02	873	171	1.38	8.21
	1	2	1	4	6000	200	150	10.9	23.2	1.26	5.52		2.73	7.91	926	172	1.32	7.94
	1	2	1	5	6000	200	150	11.5	24.3	1.17	5.88		3.37	7.70	1023	164	1.26	7.71
	1	2	2	1	6000	200	170	9.0	20.6	1.61	4.92		0.41	7.98	1773	174	1.57	9.81
	1	2	2	2	6000	200	170	9.8	24.0	1.39	5.52		0.90	8.81	1794	228	1.39	8.33
	1	2	2	3	6000	200	170	10.5	25.0	1.26	5.88		1.57	8.88	1919	239	1.29	7.67
	1	2	2	4	6000	200	170	11.3	25.3	1.16	6.24		2.57	8.62	2032	220	1.20	7.22
	1	2	2	5	6000	200	170	12.0	25.5	1.09	6.48		3.38	8.27	2129	203	1.15	7.00
	1	2	3	1	6000	200	190	10.8	22.3	1.41	5.88		0.37	8.57	3235	243	1.37	9.06
	1	2	3	2	6000	200	190	11.7	24.0	1.32	6.36		0.68	9.22	3465	298	1.25	7.97
	1	2	3	3	6000	200	190	12.7	24.1	1.18	6.84		1.41	9.35	3736	317	1.16	7.23
	1	2	3	4	6000	200	190	13.6	26.0	1.09	7.32		2.33	9.07	3952	303	1.09	6.86
	1	2	3	5	6000	200	190	14.5	27.3	1.03	7.56		3.50	8.54	4099	255	1.03	6.59
	1	2	4	1	6000	200	210	13.0	24.0	1.3	6.72		0.28	8.96	4394	299	1.26	8.61

Comments	Configuration	Test Point	Angle #	Run #	RPM	Throttle Counts	Injection Angle	Injection Quantity	Power (HP)	λ (LM-2)	Fuel Flow (kg/hr)	EGT	Emissions					
													CO (%)	CO_2 (%)	HC PPM	NO_x PPM	λ	O_2 (%)
	1	2	4	2	6000	200	210	13.9	25.4	1.17	6.96		0.53	9.53	4724	366	1.17	7.70
	1	2	4	3	6000	200	210	14.8	27.1	1.13	7.68		1.16	9.70	5132	393	1.08	6.99
	1	2	4	4	6000	200	210	15.6	27.2	1.06	7.80		2.06	9.44	5439	362	1.02	6.61
	1	2	4	5	6000	200	210	16.5	29.6	1	8.40		3.16	8.95	5717	303	0.96	6.37
	2	2	1	1	6000	200	150	10.0	31.6	1.53	5.28		0.41	9.12	579	490	1.50	8.06
	2	2	1	2	6000	200	150	10.8	31.8	1.38	5.40		0.92	9.70	479	599	1.37	6.90
	2	2	1	3	6000	200	150	11.5	32.5	1.29	5.76		1.56	9.75	435	609	1.29	6.31
	2	2	1	4	6000	200	150	12.3	33.6	1.21	6.24		2.38	9.52	433	563	1.22	5.92
	2	2	1	5	6000	200	150	13.0	33.2	1.12	6.24		3.02	9.23	449	514	1.18	5.77
	2	2	2	1	6000	200	170	9.0	26.7	1.64	5.04		0.23	8.45	831	384	1.61	9.07
	2	2	2	2	6000	200	170	10.0	31.3	1.45	5.52		0.41	9.57	725	750	1.42	7.42
	2	2	2	3	6000	200	170	11.0	34.5	1.3	6.00		1.00	10.03	694	885	1.30	6.35
Fuel cart out of fuel	2	2	2	4	6000	200	170	12.0	34.7	1.19			1.90	9.92	720	811	1.22	5.78
Fuel cart out of fuel	2	2	2	5	6000	200	170	13.0	36.0	1.1			2.99	9.48	775	665	1.15	5.49
Fuel cart out of fuel	2	2	3	1	6000	200	190	10.5	28.3	1.59			0.19	8.11	1751	240	1.59	9.78
Fuel cart out of fuel	2	2	3	2	6000	200	190	11.8	35.2	1.39			0.33	9.57	1610	814	1.38	7.68
	2	2	3	3	6000	200	190	13.0	35.8	1.26	6.60		0.74	10.09	1638	1131	1.27	6.67
	2	2	3	4	6000	200	190	14.3	37.5	1.16	7.44		1.54	10.16	1763	1153	1.18	5.94
	2	2	3	5	6000	200	190	15.5	37.9	1.09	8.04		2.90	9.59	1927	867	1.10	5.56
	2	2	4	1	6000	200	210	13.0	30.4	1.5	6.72		0.10	8.56	3074	433	1.42	9.23
	2	2	4	2	6000	200	210	14.0	34.3	1.34	7.20		0.14	9.59	3053	937	1.30	7.81
	2	2	4	3	6000	200	210	15.0	36.1	1.24	7.44		0.30	10.25	3090	1387	1.21	6.78
	2	2	4	4	6000	200	210	16.0	37.3	1.15	7.92		0.80	10.54	3220	1496	1.14	6.03
	2	2	4	5	6000	200	210	17.0	38.0	1.07	8.28		1.81	10.27	3385	1240	1.07	5.59
	3	2	1	1	6000	200	150	10.0	22.0	1.68	5.28	1070	0.73	7.59	1418	123	1.63	10.24

Comments	Configuration	Test Point	Angle #	Run #	RPM	Throttle Counts	Injection Angle	Injection Quantity	Power (HP)	λ (LM-2)	Fuel Flow (kg/hr)	EGT	Emissions					
													CO (%)	CO_2 (%)	HC PPM	NO_x PPM	λ	O_2 (%)
	3	2	1	2	6000	200	150	10.8	26.5	1.45	5.76	1135	1.06	8.54	1285	219	1.45	8.68
	3	2	1	3	6000	200	150	11.5	28.5	1.32	6.24	1155	1.62	8.77	1286	311	1.35	7.87
	3	2	1	4	6000	200	150	12.3	29.5	1.21	6.60	1150	2.40	8.60	1372	370	1.27	7.44
	3	2	1	5	6000	200	150	13.0	30.0	1.14	6.96	1140	3.18	8.27	1461	388	1.21	7.22
	3	2	2	1	6000	200	170	11.0	27.2	1.48	6.12	1130	0.49	8.61	2062	428	1.45	9.02
	3	2	2	2	6000	200	170	12.0	29.5	1.3	6.60	1140	0.89	9.14	2202	563	1.33	7.96
	3	2	2	3	6000	200	170	13.0	30.0	1.2	7.08	1150	1.84	9.10	2345	586	1.22	7.26
	3	2	2	4	6000	200	170	14.0	30.5	1.1	7.56	1140	2.97	8.67	2464	536	1.14	6.90
	3	2	2	5	6000	200	170	15.0	31.5	1.05	8.04	1120	4.20	8.05	2601	436	1.07	6.71
	3	2	3	1	6000	200	190	11.0	25.4	1.61	6.00	1040	0.19	7.97	2683	340	1.54	10.18
	3	2	3	2	6000	200	190	12.0	27.5	1.42	6.48	1095	0.25	8.85	2827	513	1.40	8.93
	3	2	3	3	6000	200	190	13.0	30.0	1.3	6.96	1135	0.58	9.50	3076	750	1.27	7.78
	3	2	3	4	6000	200	190	14.0	31.5	1.19	7.56	1150	1.42	9.56	3284	772	1.17	7.05
	3	2	3	5	6000	200	190	15.0	32.0	1.1	8.04	1145	2.42	9.20	3508	667	1.10	6.71
	3	2	4	1	6000	200	210	11.0	22.5	1.85	5.52	975	0.10	6.83	2858	116	1.73	11.82
	3	2	4	2	6000	200	210	12.5	26.1	1.52	6.24	1065	0.08	8.51	3038	437	1.44	9.50
	3	2	4	3	6000	200	210	14.0	30.5	1.28	7.20	1140	0.42	9.77	3345	890	1.24	7.54
	3	2	4	4	6000	200	210	15.5	31.2	1.13	7.92	1150	1.80	9.53	3782	704	1.11	6.77
	3	2	4	5	6000	200	210	17.0	31.7	1.02	8.76	1120	3.58	8.65	4169	401	1.02	6.48
	4	2	1	1	6000	200	150	11.0	30.0	1.5	5.64	1000	0.59	8.99	979	384	1.48	8.42
	4	2	1	2	6000	200	150	11.9	34.0	1.34	6.00	1026	1.08	9.52	996	570	1.35	7.32
	4	2	1	3	6000	200	150	12.8	34.5	1.32	6.48	1000	1.19	9.45	1021	532	1.34	7.23
	4	2	1	4	6000	200	150	13.6	34.5	1.2	6.72	1012	1.99	9.37	1060	638	1.25	6.67
	4	2	1	5	6000	200	150	14.5	35.0	1.13	7.20	1000	3.02	8.96	1147	658	1.18	6.35
	4	2	2	1	6000	200	170	11.0	32.0	1.42	6.00	960	0.33	9.14	1909	560	1.41	8.32
	4	2	2	2	6000	200	170	12.0	34.0	1.32	6.60	1000	0.59	9.76	1995	869	1.30	7.28
	4	2	2	3	6000	200	170	13.0	35.0	1.21	6.96	1020	1.12	10.02	2155	996	1.21	6.54
	4	2	2	4	6000	200	170	14.0	35.5	1.14	7.56	1025	1.92	9.83	2275	966	1.15	6.14

Comments	Configuration	Test Point	Angle #	Run #	RPM	Throttle Counts	Injection Angle	Injection Quantity	Power (HP)	λ (LM-2)	Fuel Flow (kg/hr)	EGT	Emissions					
													CO (%)	CO_2 (%)	HC PPM	NO_x PPM	λ	O_2 (%)
	4	2	2	5	6000	200	170	15.0	35.5	1.05	7.92	1010	3.04	9.34	2367	825	1.09	5.89
	4	2	3	1	6000	200	190	12.0	31.0	1.47	6.48	915	0.15	9.00	2698	598	1.40	8.74
	4	2	3	2	6000	200	190	13.3	34.0	1.32	7.08	980	0.29	9.73	2983	1027	1.28	7.60
	4	2	3	3	6000	200	190	14.5	35.5	1.22	7.80	1005	0.58	10.18	3175	1291	1.20	6.82
	4	2	3	4	6000	200	190	15.8	36.0	1.14	8.16	1025	1.36	10.26	3438	1288	1.11	6.16
	4	2	3	5	6000	200	190	17.0	37.0	1.04	8.64	1020	2.64	9.79	3681	1051	1.04	5.80
	4	2	4	1	6000	200	210	13.0	32.0	1.42	6.60	960	0.08	9.13	2960	845	1.37	8.66
	4	2	4	2	6000	200	210	14.3	35.0	1.27	7.44	990	0.17	10.19	3164	1488	1.24	7.19
	4	2	4	3	6000	200	210	15.5	36.0	1.16	8.04	1020	0.74	10.60	3409	1610	1.14	6.22
	4	2	4	4	6000	200	210	16.8	36.5	1.06	8.88	1020	2.08	10.16	3748	1165	1.05	5.72
	4	2	4	5	6000	200	210	18.0	37.0	0.98	9.24	1000	3.57	9.38	4015	732	0.98	5.53
Peak Torque	1	3	1	1	5200	1000	230	32.4	33.9	1.13			3.47	5.84	8044	167	1.04	10.25
Peak Torque	2	3	1	1	5200	1000	230	48.3	53.0	0.98			3.64	6.83	9100	545	0.93	8.82
Peak Torque	3	3	1	1	5200	1000	230	34.5	37.7	1.2	15.12	895	1.57	6.72	8889	747	1.08	10.52
Peak Torque	4	3	1	1	5200	1000	230	35.3	42.2	1.11	15.24	860	1.95	7.15	8791	1081	1.02	9.44
Peak Torque	5	3	1	1	5200	1000	230	37.6	44.3	1.06	15.48	860	2.90	6.63	8347	606	1.00	9.30
Peak Torque	6	3	1	1	5200	1000	230	36.0	43.1	1.11	14.64	877	2.50	6.70	8401	760	1.01	9.40
Peak Torque	1	4	1	1	6000	1000	230	39.2	54.6	1.1			2.16	7.38	7191	828	1.06	9.06
Peak Torque	2	4	1	1	6000	1000	230	48.3	60.5	0.96			3.74	6.65	9043	564	0.93	8.84
Peak Torque	3	4	1	1	6000	1000	230	41.1	57.5	1.16	20.88	935	1.67	7.29	7882	1126	1.08	9.73
Peak Torque	4	4	1	1	6000	1000	230	39.1	61.5	1.13	18.96	900	1.58	7.69	7061	1553	1.11	9.47